Development and Exploration of Electrochemical Cascades for Titanium-Mediated Nitrogen Reduction to Ammonia

Thesis by
Channing Klein

In Partial Fulfillment of the Requirements for the
Degree of
Doctor of Philosophy in Chemical Engineering

CALIFORNIA INSTITUTE OF TECHNOLOGY
Pasadena, California

2026
Defended 15 May 2026

Channing Klein
ORCID: 0000-0002-1593-3896

ACKNOWLEDGMENTS

Writing my thesis acknowledgments is something I often turned over in my head at night during difficult times in grad school. It's the most fun part of any thesis defense: getting to see someone finally presenting their years and years of work and then, sighing in relief, turning to the community that got them there and acknowledging them in full. But now that I'm actually here (how?), I find myself almost lost for words. It feels like too enormous a task to fully encapsulate how much I've been helped by the people around me and how impossible this thesis would have been to complete without them. Nevertheless, I'll give it a shot.

My sincerest thanks go out to every member of the Manthiram lab, past and present. Karthish, thank you for all your advice, both scientific and otherwise: I grew so much as a scientist and scientific communicator thanks to your mentorship and I'll always be grateful. Thank you also for always being open to my wild ideas (and there were a lot!) and allowing me to pursue my interests even if they sounded a bit crazy at the time. To the members of book club, thanks for the great times, good food, and excellent drinks—you all brightened some very gray days. Thanks to Emma in particular for always showing up and being the social glue that holds the lab together; to Spencer, for many commiseration sessions about French, romance, research, and everything in between; to Sundar, KP, Jeff, and Jason A. for being reliable and delightful fellow late-night crew members; to Luis and Sundar (again) for your valuable advice on cryo-TEM and help sourcing TEM grids; to Clara for many fun lab conversations (I can always count on you to be in a good mood!); to Evan for his valuable feedback on manuscripts, resumes, and everything in between; and good luck to the first years—I know we're leaving the lab in good hands!

I'm also incredibly grateful to my subgroup. Sub Li and Sub N (past, present, and future!), you will always be famous—thanks for your unwavering support, your humor, your uncomplaining teamwork, and your INCREDIBLE scientific expertise. I learned so much being a member of this subgroup and you all made every day in lab better. Gangsan, you are an incredible mentor and one of the hardest-working and kindest people I've ever met. Thank you for keeping our gremlin-infested glovebox on life support and for all your advice and help! Michael, you are one of the smartest people I know, and also the most generous with your time—your thorough and analytical approach has made me a better scientist. Thank you for always being a delight to hang out with! Anukta, you are a bright spot of joy in the lab—you're

literally always so cheerful and kind and it makes my day better to see you around the office. Thanks for being a great project partner! And Curtis, I wish you the best of luck with your Ph.D. It's been great getting to know you, even for a short time, and I'm excited to see how you carry TiNRR forward!

I had the privilege of mentoring two undergrads over the course of my PhD, Erin McMurchie and Alexis Lindenfelser. Both are incredibly bright, creative, and hard-working students and it was nothing but a pleasure to work with them. Erin, you joined our lab at an incredibly chaotic time (we had just moved to Caltech and were moving lab spaces!) and were paired with an incredibly chaotic mentor (first-year me) and you handled all of this with grace and fortitude. Thank you for your patience with me and willingness to engage with our project on a deep level—I'm so proud of what you achieved with us and all you've done since then! Alexis, having you as a project partner made coming to lab worth it. You are terrifyingly smart and devastatingly competent; chapter 2 of this thesis would have been impossible without you. Thank you for your patience with my rambly explanations and truly horrific work schedule; your jokes and good cheer made every day better. Never stop believing in yourself—I'm so excited to see what you achieve next!

Thank you also to the MIT alumni of the lab who overlapped with me: Zach, Nathan, Kindle, Joy, Minju, Joseph, Hee Jo, and Katie. Joy, Minju, and Joseph spent the most time with us; you three handled a difficult transition with incredible grace and I learned so much from all three of you. Thank you so much for sharing your expertise with us first years, even from far away. Kindle, your passion and big heart are a true inspiration; in my first year, all I wanted was to be like you when I graduated. I hope I've succeeded even a little bit. Hee Jo, thank you for your generous mentorship and time—you helped me set up my first-ever GDE cell over the phone from MIT! You went above and beyond as a mentor and I am very grateful. Katie, you are one of the most rigorous, careful, and intelligent scientists I've ever met. Your approach to research continues to inspire me to this day. Thank you for all the time you spent on video call with me helping set up experiments and understand LiNRR. You've already accomplished incredible things and I look forward to seeing what you do next!

I also need to acknowledge the many other mentors who have helped me along the way. Haochen, you're smart, blunt, and always manage to cut right to the core of whatever problem I'm struggling with. Thank you so much for your generosity, support, and kindness. Gangsan, I already thanked you above but I can't overstate

how much your steady work and expertise has helped me. Wes, thank you for for your excellent advice and help in navigating the world of industry. Rachel, thank you for being an incredibly kind and understanding voice of reason in the chaos of first year. I'm incredibly grateful also to the members of my committee, Kim See, Julia Greer, and Zhen-Gang Wang. Each of you have supported me at different times throughout grad school and I couldn't have made it here without your advice and encouragement. Finally, shout-out to Nate Siladke, Nathan Dalleska, and David Vander Velde for helping out with various aspects of safety and instrumentation—it's been a huge privilege to be able to work with experts on my project!

Of course, I wouldn't have even made it here without a fantastic undergraduate lab experience that entirely altered my career trajectory. As an undergrad, I worked in Ian Tonks' lab at the University of Minnesota, and I'm so glad to have met every single person there. Ian, thank you for being a kind, understanding, and rigorous mentor. You held me—all of us in lab—to a high but reasonable standard that was so helpful in assessing my own graduate work and setting realistic goals for myself. You went to bat for me so many times; without your advocacy and recommendations, I couldn't have afforded to do research and would not be here today.

Thanks also to my two mentors in the Tonks lab, Yukun Cheng and Xin Yi See. Yukun was brave enough to take me on as a freshman and taught me most of what I know about airfree lab techniques—Yukun, thank you for your patience with me throughout myriad lab accidents and dumb questions and for taking the time to help me truly understand the science we were doing. Xin Yi, you are brilliant, generous, and wise, and I am privileged that I got to be your mentee in your last year of grad school. Thank you for your advice, now and then (my job search wouldn't have been nearly as successful without you!) and helping me develop realistic expectations of my own research. Also, thank you to Connor, Steven, Janaya (and Brady!), Robin, Evan, Abby, the Rachels, Ben, and Dan for support, encouragement, and genuine friendship. I'll always be grateful.

I genuinely don't know that I would be alive today without the other members of my Manthiram lab cohort: Chenyu, James, and Thu. This group of friends has been there in the worst times and the best. They've brought me food and meds when I was sick, dragged me out for ice cream when I was sad, cared for my cats, and shared their hopes, thoughts, and dreams. I am genuinely so incredibly honored and happy to be a person these incredible souls want to be around (!!!) and to have made so many wonderful memories with them.

Chenyu, you are passionate, strong, and brave, a rigorous scientist with a keen mind and a huge heart. Your strength in the face of adversity, your steadfast commitment to your principles, and your kindness and compassion for both animals and people inspire me every day and will continue to do so. You've been a constant presence in grad school, from our first year rooming together to our last year living in the same apartment building. You're an incredible mama to your cats and the perfect auntie to mine. I am so, so grateful for all the time we've spent together driving, ice skating, concert going, and just hanging out complaining. I can't wait to see what you achieve next! Also, shout-out Ziggy and Louie for being the best cat nephews, I love you Ziggy and Louie!!

James, it's been a wild ride from start to finish. You're so adventurous that it's inspired me to take more risks too—thanks for taking me climbing and to the arcade, for always being down for random little adventures (I'll never forget us walking an entire box spring across Pasadena!), for broadening my taste in books, movies, and podcasts, and for letting me crash at your place in NYC on one particularly memorable weekend. Your passion for science and boundless curiosity always inspire me to see the world around me with new eyes. You are funny, sharp, and incredibly selfless. I wish you the absolute best and I know that you're going to go on to even greater things.

Thu, you have been a steady rock throughout grad school. You never lose your sense of perspective and that has been a lifeline in many ways. It has been so nice to be able to just hang out and chat, in the office, in the lab, at coffeeshops and ice cream parlors and restaurants, on the way to the beach, and chasing feral cats around apartment buildings (hopefully that one won't be repeated!). You're so easy to talk to and your perspective is always wise, common-sense, and compassionate. You're generous in friendship to an extraordinary degree—with your time, your attention, your sympathy, and your resources. I feel incredibly privileged to have experienced this and for all the time we got to spend together, and I wish you all luck, happiness, and success.

My other grad school friends also deserve far more thanks and acknowledgment than I can ever express. Kim, Conner, Colin, and Logan helped to turn grad school from a harrowing trial by fire into something of a home. Kim, Conner, and I met in first year when we were all organic chemistry grad students; only Kim stayed that course, but somehow us three have remained friends through it all. Kim, your work ethic is matched only by your boundless passion for chemistry and your huge capacity for

love. You are a true friend and our long chats outside Schlinger will always remain a fond memory. Conner, you have persevered through some of the toughest challenges grad school can throw at a person, and your strength and steadfastness continue to inspire me. The money we three have spent on boba over the years would probably have been enough to open our own boba shop, but I don't regret a bit of it.

I met Colin in first year, and then we simply ran on parallel tracks until this year, when suddenly, serendipitously, we became friends. Colin, my only regret is that we didn't start this friendship sooner. You are such a generous, thoughtful, and genuinely insightful person. Spending time with you is a rare pleasure: there aren't many people I'd be happy to wander around a mall with for hours, but somehow we can talk as if we grew up together. Knowing you is a privilege, and one I hope continues all my life.

Logan and I should have met far earlier than we did. We went to the same undergrad, majored in the same field, took the same classes, even worked in the same building…but UMN is so big that we somehow missed each other until after graduation, when we both saw that someone else in our class was going to Caltech. Logan, I cannot express how glad I am that we met. You were my first friend here and have remained my best friend through twists and turns neither of us could have anticipated. I've never met someone who is so exactly on my wavelength: someone I can talk to about anything and who I can understand without words. From dragging each other on runs in our first year to our Vegas road trip to hikes and concerts and many banger restaurants, our times together are some of the brightest points of the last five years. Our interests are so different, but I literally never get tired of hearing about your life, your new hobbies, new facts you've learned—anything and everything. Thanks for educating me about books, Korean food, some incredibly strange video game strategies, what to look for in a good bike, geography, history, and random gossip. Your intelligence, boundless curiosity, sense of humor, kindness, and strength through adversity never cease to amaze me. It's been a privilege to know you and I look forward to seeing where life takes the both of us!

My friends outside of grad school have been a constant reminder that academia isn't all there is and that there are many paths to a rich and full life—a reminder that has been sorely needed at times over the past five years. I'd particularly like to thank Caspian, Anna, Noldo, and Frankie here for their friendship and kindness. Caspian, your creativity, kindness, and nuanced perspectives have changed the way I think. It's been such a pleasure to get to know you, to get to read your writing and have

my mind blown about theology and history, to learn about various fibercrafts and dances, and to learn what life is like on the humanities side! I'm so proud to be able to count you as a friend. Anna, exchanging postcards with you has been such a joy. Thanks for sharing your writing, translation expertise, and wisdom with me. Noldo, it has been a delight and a privilege to get to know you and watch you grow and mature; you are a wonderful friend and gifted artist. I cannot wait to see where life takes you next!

Frankie, we met at a difficult and dark time of my life, and you lit it up like an explosion. I'll never forget reading your writing for the first time and thinking *wow, this author is incredible* and then getting to chat with you and realizing you were also one of the nicest people I've ever met! Being creative with you reignited a spark inside me that I thought was long dead—if I enjoy creative writing today, if I ever sit down and make art for art's sake, it's because of you. And not only that—you've also been a real and genuine friend. You were there for me on some of the hardest days I've had. You're always willing to listen and share sympathy and advice. We have so much in common and getting to know you better has been a great joy. I look forward to being in the same time zone! Also, shout-out to ghosti and lena for being fantastic writing partners and friends—you all are true artists.

I also want to acknowledge a few people who are no longer in my life. These are people—ex-friends, ex-partners—who were there for me during some of the worst times of my life and kept me sane, who taught me what it was to be cared for and seen. They left my life for a variety of reasons, some tragic and some very mundane, but it's important to me that they be acknowledged anyway. So: Jacob, Sarah, Lizzy, Echo, Kate, Ashwani, Jamie, Evie: thank you.

My family has been there for me in many ways over the last five years, and I'm so grateful to them as well. Mom, thank you for many delightful and calming chats—you're the best part of going to the grocery store! Thanks for always being there over the phone when I needed you, even when it was 3am. Dad, thanks for coming to pick me up at five in the morning and for being willing to talk even when we disagree. Valerie, thanks for the check-ins and for consistently making space in your busy schedule to hang out with me. I always enjoy it and your thoughtfulness means a lot. (And all love and gratitude to Portia and Roland—gone but always treasured—and Oswin and Blue, for being the wonderful cat heroes who got me through undergrad.) Grandma and Grandpa, thanks for always being down to chat on the phone, for wonderful meals and time spent on puzzles, games, and just hanging

out (and to Quint, Diamond, Martigan, Jilly, and Fancy, more cats who have made my life brighter. Quint, Diamond, and Martigan live on in my heart and memories). Heather (and co!), thanks for your love, support, and fabulous coffee machine—it means a lot when you make time for me. And of course, thank you to Princess Twilight Sparkle (Twilight for short) for being the best dog in the world.

My siblings get their own paragraph—there's too much to say and not nearly enough space to say it in, but I'll give it a go. Berit, thanks for coming to visit and weathering a hurricane (!) with me. It's been wonderful getting to know each other as adults! Aleksander, you drove all the way out to California with me, helped me unpack and go grocery shopping, and were there for me during the first few days when my life felt like utter chaos. Thank you bro and I'm so proud of you. Bjorn, I have no idea how our family produced someone so charming, but I'm glad there's at least one of us—thanks for all the jokes and late-night poker. Colson, it's been wonderful getting to watch you grow up (even from afar) the last five years; you have grown into a generous, humorous, and thoughtful person and it's always a genuine delight to hang out. Kiri, thank you for being one of the top sisters of all time. You are sweet, kind, artistic, talented, and smart. Thanks for hanging out with me, sharing your interests (and getting into mine! It was so fun to go see Twice together!), your thoughts, your emotions, your art (I treasure your letters), and your boundless energy. Last but CERTAINLY not least, Jascha, you are an utter delight and I love hanging out with you! Thanks for all the games of Mario Kart, Smash, and even Strikers, for keeping me up to date on the latest memes, and for your constant encouragement and curiosity. I love you all.

Finally, this section wouldn't be complete without an acknowledgment of the beloved creatures who live with me: my cats, Momo and Purrseus. I met Momo in my second year of graduate school. He was two years old and severely traumatized; he was on the same anxiety meds as me and refused all touch. I fell in love sight unseen and took him home. It took three months for him to come out of his hiding place while I was in the room, longer still for him to allow me to pet him, but it was all so, so worth it. He's become a total cuddlebug and snuggles with me every night. He shoos me to bed when I'm up too late and happily comes to hang out any other time of day.

In my fourth year of grad school, I thought Momo seemed lonely, so I went to Pasadena Humane looking for a kitten. My first sight of Purrseus, he was furiously meowing and climbing the bars of his enclosure. Halfway up, he fell straight into his water bowl, but that only dampened his body and not at all his moral outrage: he

continued to yell the entire time I was visiting. Of course, I had to take him home, where he immediately tried to climb the side of my tub and fell straight into his water bowl again. He is playful, mischievous, and impossible not to love, and gets along with Momo better than I ever thought possible. So thank you to Momo and Purrseus for being there with me in grad school: living with you two is a privilege and a joy. I love you more than I could ever express.

ABSTRACT

The Haber-Bosch process, invented at the turn of the 19th century, revolutionized agriculture by providing a way to make ammonia—an important component of fertilizer—from nitrogen and hydrogen. It's been estimated that without artificial ammonia synthesis, up to half the population would starve. However, this miracle chemistry comes with costly downsides, responsible for the consumption of an estimated 2% of global energy and for up to 1.6% of global carbon dioxide emissions. Therefore, the development of new methods of ammonia synthesis that are compatible with a greener society is a task of paramount importance. In this thesis, one such method for doing so—an electrochemical cascade reaction involving a plated alkali metal and a homogeneous titanium compound—is developed and explored. Electrochemically-generated sodium naphthalenide in conjunction with titanium isopropoxide is shown to enable a high rate of ammonia synthesis, but low selectivity. By contrast, potassium metal with titanium isopropoxide allows for much higher selectivity at the cost of rate. It is found that the rate-determining step of these reactions is usually electrochemical reductant generation, a powerful discovery that allows for precise tuning of rate via changing applied current density. This spatially-decoupled reaction paradigm is also applied to other alkali metal and transition metal compounds in order to open up a wider chemical space. While much remains unknown about the mechanism of this system, the novel reactivity demonstrated in this work will have immense impacts on the field of sustainable ammonia synthesis.

PUBLISHED CONTENT AND CONTRIBUTIONS

(1) Klein, C. K.; Lindenfelser, A.; Yusov, M. A.; Jain, A.; Jones, R. J. R.; Gregoire, J.; Manthiram, K. *Joule* **2025**, *9*, 101923,
C.K.K. conceived the project, collected and analyzed the data, and wrote the manuscript.

TABLE OF CONTENTS

LIST OF ILLUSTRATIONS

LIST OF TABLES

NOMENCLATURE

$Al(O^iPr)_3$. Aluminum isopropoxide.

$AlCl_3$. Aluminum chloride.

Cp_2TiCl_2. Titanocene dichloride.

DME. Dimethoxyethane.

EPR. Electron paramagnetic resonance spectroscopy.

EtMgBr. Ethylmagnesium bromide.

EtMgCl. Ethylmagnesium chloride.

FE. Faradaic efficiency.

GHG. Greenhouse gas.

HER. Hydrogen evolution reaction.

IPA. Isopropyl alcohol.

KIE. Kinetic isotope effect.

KO*t*Bu. Potassium tert-butoxide.

$LiAlH_4$. Lithium aluminum hydride.

$LiBF_4$. Lithium tetrafluoroborate.

LiDFOB. Lithium difluoro(oxalato)borate.

LiF. Lithium fluoride.

LiNRR. Lithium-mediated nitrogen reduction reaction.

LiTFSI. Lithium trifluoromethanesulfonate.

NaNp. Sodium naphthalenide.

NTP. Normal temperature and pressure, defined as 1 atm of pressure and a temperature of 298.15 K.

RE. Reference electrode.

SEI. Solid-electrolyte interphase.

SMR. Steam methane reforming.

TBACl. Tetrabutylammonium chloride.

$Ti(O^iPr)_4$. Titanium tetraisopropoxide.

$TiCl_4$. Titanium tetrachloride.

TiNRR. Titanium-mediated ammonia synthesis.

WGS. Water-gas shift.

Chapter 1

INTRODUCTION

Life on Earth as we know it could not be sustained without artificial ammonia synthesis. Ammonia (NH_3) is an essential fertilizer; without the ammonia currently produced from nitrogen and hydrogen in the Haber-Bosch process, approximately three billion people would starve.[1] Additionally, ammonia is a vital reagent for organic synthesis in many forms; it serves as an acidity-modifying solvent as well as a nucleophile that forms a building block for many different functional groups.[2] As of 2022, global production of ammonia by mass was 150 million metric tons; and to further drive home its importance, it is the only reaction to have won three Nobel Prizes in Chemistry (in 1918, 1931, and 2007).[3,4]

1.1 The Haber-Bosch process

Chemistry and Operation

Over 90% of ammonia is currently produced by the Haber-Bosch process,[5] which combines N_2 and H_2 over an iron or ruthenium catalyst to form ammonia via the following reaction:

$$0.5\,N_2(g) + 1.5\,H_2(g) \rightleftharpoons NH_3(g) \tag{1.1}$$

Ammonia formation via this method is exothermic by 46.1 kJ mol^{-1} at NTP. Thus, it is favored thermodynamically at high pressures and low temperatures. At ambient temperatures, the reaction is too kinetically sluggish to produce significant amounts of product; therefore, it is necessary to apply both high temperature (to increase rate of reaction) and high nitrogen and hydrogen pressures (to shift the equilibrium towards ammonia). Due to these fundamental limitations, modern Haber-Bosch plants operate at 350–450 °C and 100–200 bar.[6]

However, even these conditions are not sufficient for a single-pass conversion of more than 15%, necessitating recycling the remaining feedgas multiple times.[7] This increases the energy intensity of the process; a typical energy efficiency for the Haber-Bosch process is around 65%.[8] Overall, the process is able to achieve up to 97% conversion after multiple passes.[7] This demonstrates that proper reactor and process engineering is just as important than development of a chemical reaction

itself, and will be a major component of future efforts at sustainable ammonia synthesis.

The way in which the feedgas is prepared is also of importance. Nitrogen is isolated from air via cryogenic distillation, followed by filtration to obtain ultra-pure nitrogen feedstock. This is necessary as oxygen poisons Haber-Bosch catalysts.[6] Hydrogen is produced via steam methane reforming (SMR):

$$CH_4(g) + H_2O(g) \rightleftharpoons 3\,H_2(g) + CO(g) \tag{1.2}$$

SMR is highly endothermic (ΔH^0 = +205.9 kJ mol^{-1} at 298 K) and thus is operated at temperatures between 500–900 °C and pressures >20 atm.[9] Following this step, the syngas produced undergoes the water-gas shift (WGS):

$$CO(g) + H_2O(g) \rightleftharpoons CO_2(g) + H_2(g) \tag{1.3}$$

WGS is slightly exothermic (ΔH^0 = -41 kJ mol^{-1} at 298 K), so this reaction is typically run at 350 °C. Finally, pressure swing adsorption is used to purify the resulting H_2.[9]

Environmental issues of the Haber-Bosch process

The Haber-Bosch process poses an immediate and grave threat to the environment. By itself, it is responsible for 1.2% of global anthropogenic CO_2 emissions.[1,10] 50% of Haber-Bosch plants produce ammonia using methane as a feedstock. The SMR/WGS process has been estimated to produce 13.7 kg CO_2/kg H_2 when methane is used as feedstock, representing approximately 76% of the CO_2 emissions from the Haber-Bosch process.[11–13] The remaining 24% of emissions in this case occur from the burning of methane to provide the heat necessary to form ammonia.

Utilization of methane is the current best-case scenario for Haber-Bosch emissions; the other 50% of Haber-Bosch plants utilize oil (31%) or coal (19%), both of which produce significantly more greenhouse gas (GHG) emissions than methane.[8] Additionally, calculations of the GHG emissions associated with the Haber-Bosch process ignore the environmental impact of natural gas extraction, which pollutes the air and destroys natural ecosystems.[14]

Socioeconomic issues of the Haber-Bosch process

Because Haber-Bosch plants must be capable of producing high temperatures and extreme pressures, and require large amounts of fossil fuels to run, they are extremely capital-intensive. Thus, there are fewer than 100 Haber-Bosch plants worldwide, largely concentrated in North America, Europe, China, and India.[15] This results in disproportionate costs of fertilizer in developing countries, which in turn means that typical fertilizer use across Africa is an order of magnitude less than the global average. For example, in Sierra Leone, fertilizer use has been estimated at 4 kg/ha, compared to the global average of 100 kg/ha. This has contributed to a significant agricultural output deficiency: 50% of households are food insecure.[16]

Additionally, a large portion of electricity in developing countries is generated by renewable sources such as hydroelectric or wind. For example, across Africa, hydroelectric power accounts for at least 17% of the total electricity generated.[17] Because hydroelectric power is by nature intermittent and weather-dependent, it is exceptionally difficult to develop the infrastructure for an energy-intensive process like Haber-Bosch in these developing countries. Thus, the Haber-Bosch process actively contributes to global inequality and food insecurity.

Finally, the events of the last five years have brought into sharp relief the importance of decarbonized technology for fertilizer production. The United States' recent invasion of Iran as well as the ongoing Russia-Ukraine war demonstrate the risks of being completely dependent on natural gas for agriculture. In October 2022, just 8 months after Russia's invasion of Ukraine, roughly 70% of European ammonia production was shut down or reduced due to the sudden increase in natural gas prices.[18] Meanwhile, the ongoing blockade of the Strait of Hormuz is impacting both natural gas and ammonia availability, particularly in South Asia.[19] A method of producing ammonia that is not dependent on global politics and is compatible with intermittent energy sources is thus a matter of some socioeconomic urgency.

1.2 Electrochemical ammonia synthesis

Electrochemical ammonia synthesis offers solutions to both the environmental and socioeconomic problems posed by the Haber-Bosch process. It can be performed at ambient temperature and atmospheric or slightly-elevated N_2 pressure, effectively doing away with the quarter of emissions associated with generating the extreme conditions required for Haber-Bosch catalysts to work. Many electrochemical ammonia synthesis conditions utilize mild organic acids rather than hydrogen as a pro-

ton source for ammonia. While this poses its own environmental problems, it does do away with the necessity of methane steam reformation. If hydrogen is used as a proton source, it can be synthesized electrochemically using a water electrolyzer, which is feasible on the small, localized scale envisioned for electrochemical ammonia synthesis processes.[20]

Because electrochemical ammonia synthesis can operate on a smaller scale, and intermittently, it is ideally positioned to address the socioeconomic inequalities engendered by the Haber-Bosch process as well. A hypothetical small-scale electrochemical ammonia synthesizer would require a much smaller upfront capital investment, making it more accessible to farmers who currently cannot afford the fertilizer they need. Additionally, because the process operates at ambient temperature and thus can be stopped and started without enormous efficiency losses, the technology is compatible with even very intermittent electricity sources, offering the ability to synthesize ammonia in places where access to electricity is inconsistent.

Li-mediated electrochemical nitrogen reduction (LiNRR)

LiNRR was initially discovered in the 1930s by Erlenmayer, and rediscovered in the 1990s by Tsuneto et al.[21–23] The technology was fully verified in the late 2010s, and has advanced rapidly since then as a result of increased interest in sustainable ammonia production.[24,25] Faradaic efficiencies (FEs) of 100% have been reported at 15 bar, and nearly 100% FE has been achieved at ambient pressure.[26–28] Despite these significant advances, the system has many disadvantages that currently hinder its commercial viability.

The mechanism of LiNRR has yet to be fully elucidated. However, the commonly-accepted mechanism involves Li metal—the only catalyst that can spontaneously split nitrogen at room temperature—being electrochemically plated. This metal thermochemically reacts with nitrogen to form Li_3N. This intermediate then reacts with a proton donor—usually present in solution—to give ammonia and regenerate Li salt, as shown in Fig. 1.1.[24]

The two main processes competing with ammonia formation are Li plating and the hydrogen evolution reaction (HER).[29] If Li plates too quickly, not all plated Li is used to reduce N_2, resulting in FE losses and an eventual buildup of Li on the electrode. However, by far the most parasitic process is HER. Hydrogen evolution occurs thermochemically due to the reaction of Li with protons in solution. It also occurs electrochemically, at a much more positive potential than Li plating (0 V vs. NHE,

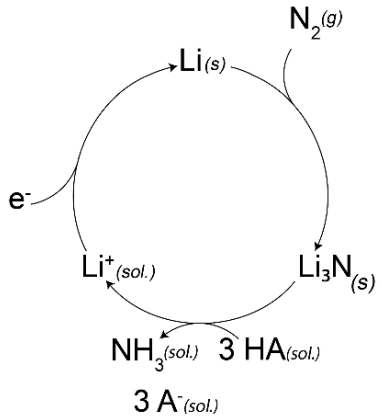

Figure 1.1: Postulated mechanism of LiNRR.

as opposed to -3.04 V vs. NHE for Li plating).[30] Protons must be present in solution for ammonia to be formed, so they cannot simply be removed from the system entirely. Thus, enabling Li plating while avoiding HER is a challenging problem.

The most common approach taken by research groups to address this issue is minimizing the activity of protons present in solution while maximizing the activity of N_2. Proton activity is commonly reduced both by using the minimum quantity of proton donor necessary and utilizing a relatively-basic proton donor such as ethanol or a similar alcohol.[31,32] Effective N_2 concentration can be increased either by the use of a gas diffusion electrode to reduce boundary-layer thickness at the electrode, or by simply increasing N_2 pressure.[33]

Complicating the system is the existence of the solid-electrolyte interphase (SEI), an ionically-conducting, electronically-insulating layer which forms on top of metallic Li.[34] Originally investigated in the context of Li-metal batteries, the SEI has been identified as a key player in the transport of N_2 to the plated Li, and hence has a large impact on the kinetics of the system. If the SEI is too "protective," neither nitrogen nor protons reach the Li metal, and it becomes totally inert. Indeed, Manthiram and co-workers found in 2023 that without a proton donor present in the system, N_2 is prevented from reacting with Li. By contrast, if the SEI is too porous, HER dominates and no ammonia is formed.[35]

Recent efforts to improve selectivity towards ammonia in LiNRR have focused on electrolyte and electrode engineering. At high pressure, two separate works have achieved 100% or near 100% FE. MacFarlane and co-workers achieved 100% FE utilizing a lithium trifluoromethanesulfonate (LiTFSI) electrolyte and 15 bar N_2.[26] They attribute the remarkable success of their system to the stability of the $TFSI^-$

anion under strongly reducing conditions, resulting in a very thin SEI. They also postulate that the ability of the $TFSI^-$ anion to facilitate fast Li^+ transference at the electrode-electrolyte interface is key to the excellent performance of their system. However, it is unclear how many of their conclusions are valid at ambient pressure.

By contrast, Chorkendorff and co-workers—also at high pressure—utilized a $LiBF_4$ electrolyte to achieve nearly 100% FE at 20 bar N_2.[27] Remarkably, they also achieved a current density of -1 A cm^{-2}, which is over an order of magnitude larger than any group has demonstrated. Their success is attributed to the BF_4^- counteranion breaking down to form a LiF-rich SEI that facilitates efficient transport of both Li^+ and N_2 to the electrode surface. Interestingly, this conclusion contradicts that of MacFarlane et al., who have written that unstable counteranions such as BF_4^- necessarily result in lower FEs and a highly unstable system. Chorkendorff et al. also demonstrated 67% FE towards ammonia from N_2 and H_2 at ambient pressure with the use of a continuous-flow system.[36] They utilized gas diffusion electrodes to overcome N_2/H_2 transport limitations. Besides the significant achievement of nearly 70% FE towards ammonia at ambient pressure, the group also showed that at least 50% of produced ammonia was in the gas phase, significantly simplifying the separation process.

Finally, just this year, 98% FE towards ammonia in LiNRR was demonstrated at ambient pressure, along with a record energy efficiency of 21%.[28] The authors hypothesized that in a system with sufficiently optimized nitrogen transport through the SEI to the lithium surface, the reaction becomes limited by diffusion of lithium ions through the SEI. After performing theoretical calculations to determine factors affecting the rate of reaction, they utilized a Li difluoro(oxalato)borate (LiDFOB) electrolyte in THF in order to form an SEI rich in LiF, which they hypothesized to enable faster Li diffusion to the surface. Indeed, they found that this was the case, and achieved 98% FE (80% over 40 hours). Due to the increased diffusion coefficient of Li ions, they were also able to reduce the cathodic overpotential significantly and achieve 21% EE.

Despite the remarkable progress in recent years towards developing LiNRR, the system has serious flaws that make industrial viability challenging. First, the system as a whole has a hard cap on energy efficiency (EE) of 38% due to the extremely negative potential of Li plating.[24] This is not an insurmountable hurdle at small scale, but the maximum EE of nonaqueous LiNRR is likely to be much lower than that due to the high resistance of nonaqueous electrolytes. The highest EE ever achieved for

LiNRR, cited above as 21%, requires a 2 M solution of LiDFOB, an expensive fine chemical.

Cost is another important metric which LiNRR currently fails. Demand for Li is growing exponentially due to rising demand for Li-metal and Li-ion batteries, which are vital for grid storage, electric vehicles, and many other renewable energy applications.[37] Although significant strides are being made in battery recycling and electrochemical lithium extraction, the market is still susceptible to sudden swings and peaks in prices as lithium supply remains ill-equipped to meet sudden increases in demand.[38]

1.3 Titanium-mediated ammonia synthesis

The first example of the use of titanium for nitrogen reduction to ammonia (TiNRR) was published in 1964 by Vol'pin and Shur,[39] with an English follow-up in 1966.[40] Motivated by the known activity of metal centers in biological nitrogenases and the (at the time) recent discovery of the ability of molybdenum and tungsten complexes to fix nitrogen,[41] the authors screened a variety of transition metal complexes (including chromium, iron, and titanium) and reductants (primarily $LiAlH_4$ and EtMgBr). Upon initial testing, they found that $TiCl_4$ with EtMgBr at 150 atm of nitrogen gave a 10% yield of fixed nitrogen vs. Ti (Fig. 1.2a). However, switching from $TiCl_4$ to the more electron-rich complex Cp_2TiCl_2, the authors were able to demonstrate 100% conversion of nitrogen vs Ti at 150 atm (Fig. 1.2b). More strikingly, they were able to reach a 70% yield at atmospheric pressure. Both these results were an order of magnitude higher than all other metals and conditions screened.

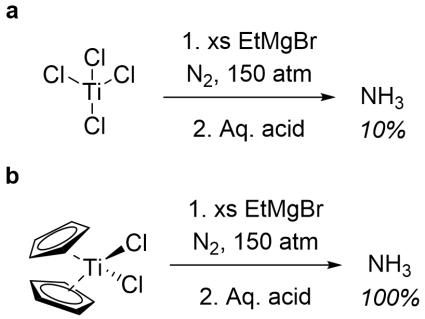

Figure 1.2: Results of Vol'pin and Shur's initial studies on Ti-mediated nitrogen reduction.
a) Reduction reaction using $TiCl_4$.[39] b) Reduction reaction using Cp_2TiCl_2.[39]

These results kindled interest in titanium- and particularly titanocene-mediated ammonia synthesis; the following year, Hans Brintzinger published a two-part EPR

study on nitrogen reduction at Cp_2TiCl_2 using EtMgCl.[42,43] He proposed a hydride-mediated mechanism, wherein the Grignard reagent first attacked the Ti center to form MgCl and a Ti alkyl, which then underwent an elimination reaction to give ethylene and a Ti hydride dimer (Fig. 1.3a).[42] The next year, Brintzinger revised his thesis after a more detailed EPR study, concluding that the Ti hydride was in fact a monomer (Fig. 1.3b).[44] Two years later, Henrici-Olivé concluded, based on their studies of reactivity, that the "monomer" observed by EPR as a result of reduction by Cp_2TiCl_2 by Grignard reagent was in fact an asymmetric dimer (Fig. 1.3c).[45]

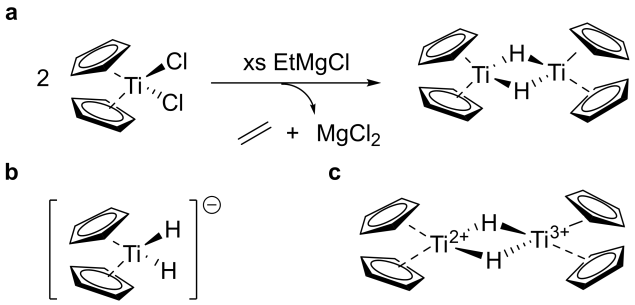

Figure 1.3: Brintzinger and Henrici-Olivé's hypothesized Ti hydride structures. a) Initial reaction and structure proposed by Brintzinger in 1966.[42] b) Hydride monomer proposed by Brintzinger in 1967.[44] c) Asymmetric hydride dimer proposed by Henrici-Olivé in 1969.[45]

However, the hypothesized behavior of this hydride complex is not compatible with other mechanistic evidence gathered around this time. In 1967, Maskill and Pratt performed a kinetic study on the Cp_2TiCl_2/Grignard system.[46] They found that the concentration of reductant was important until 0.66 M (16 equiv per Ti in their system), after which the concentration became unimportant. Based on this result and their observations of color changes at the beginning of the reaction, they hypothesized that the reaction between EtMgBr and Cp_2TiCl_2 was very fast and occurred before any nitrogen reduction steps had occurred. However, the proposal that 16 equivalents of reductant are necessary to reduce one Ti compound before any nitrogen reduction can occur is somewhat far-fetched. The authors are likely correct that *a* reduction reaction between EtMgBr and Ti is occurring independent of the other steps (particularly since they observe the same type of color change and effervescence regardless of whether nitrogen is present), but EtMgBr probably plays a more complex role in the reaction.

In addition to this, Maskill and Pratt also found a dependence on nitrogen partial pressure, which appeared to follow saturation-type kinetics: at low nitrogen partial

pressures (≤ 0.5), the partial pressure strongly affected the reaction rate. However, above these pressures, increasing partial pressure had no effect. Additionally, they uncovered a second-order dependence on Ti concentration at 1 atm nitrogen partial pressure. This suggested the existence of two distinct regimes: the low-pressure regime (N_2 partial pressure ≤ 0.5), where the rate-limiting step involved nitrogen, and a high-pressure regime (N_2 partial pressure ≥ 0.5) where the rate-limiting step was dictated by Ti concentration. This also suggested that the active form of the titanium species was a dimer of some sort. From this, and from the previously-reported fact that in this system, ammonia is not formed before quenching (thus ruling out a hydride-related mechanism of ammonia formation),[47] the authors concluded that the titanium hydride identified by Brintzinger was likely a minor byproduct rather than the major reactive species. This has been borne out by the subsequent literature, in which titanium-hydride-mediated nitrogen reduction has not been proposed since.

Exploration of the titanium reductant came next, and proved a major breakthrough for the field. Dr. Eugene van Tamelen is better known for the first synthesis of Dewar benzene,[48] his contributions to biomimetic chemistry,[49] and for being the mentor of Barry Sharpless.[50] However, he was also an immense force for progress in TiNRR development, publishing 7 papers over only three years (1967 – 1970).[51–57] His first major innovation was the use of titanium alkoxides rather than titanocenes.[54] In situ generation of di-tert-butyltitanium(IV) chloride was accomplished by mixing $TiCl_4$ with two equivalents of KO*t*Bu under nitrogen at ambient pressure; to this solution was added two equivalents of potassium metal to reduce the titanium species (Fig. 1.4). This system was remarkable for being the first titanium-mediated nitrogen reduction which did not require quenching to produce ammonia; that is, ammonia was produced in situ and was detected in an acid trap downstream of the reactor. The yield of this volatile ammonia was 10-15% (relative to Ti) over three weeks: a slow rate, but an immense conceptual step forward, as in situ production of volatile ammonia meant that in theory, the active site could be turned over.

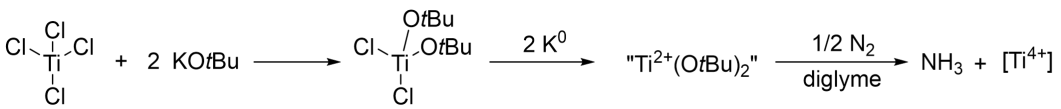

Figure 1.4: Initial titanium-mediated nitrogen reduction system by Van Tamelen and coworkers.[54]

Two major hypotheses were put forward in this work which have remained foundational to the field. First, the researchers observed that two full equivalents of potas-

sium were required to initiate ammonia synthesis. When only one equivalent was added, no ammonia was detected. From this, the authors concluded that titanium(II) must be involved in the nitrogen reduction reaction, as shown in Fig. 1.4. This observation (that two equivalents of reductant are required to begin TiNRR) has been repeated in different experimental settings.[52,56] However, the exact reason for this observation remains unclear. It may be that, as van Tamelen and coworkers speculated, Ti(II) is the active species for ammonia synthesis. However, there are other possibilities. One alternative hypothesis is that the first equivalent of reductant is required to generate Ti(III), which then binds nitrogen. The bound nitrogen could then be reduced by the potassium metal. It also remained unclear what the source of the third electron for this three-electron reduction process was.

The second major hypothesis was that the source of protons for ammonia formation in systems wherein ammonia is released before the addition of a proton source such as acid or water is the ethereal solvent.[54] Reactions run with careful precaution taken to remove all adventitious water did not show any decrease in yield, while reactions run in non-ethereal solvent—such as benzene or xylene—did not produce any ammonia without addition of an outside proton source. Additionally, the identity of the alkoxide ligands on Ti did not appear to affect yield significantly, suggesting that the proton source is not the alkoxides. Intriguingly, this suggests that ethereal solvents such as THF or DG are simultaneously poor proton donors for hydrogen evolution at alkali metals and competent proton donors for reduced nitrogen-titanium species.

Despite all this mechanistic murkiness,[58] van Tamelen and co-workers were able to push this system's performance significantly higher. Their first innovations were enabling a) catalytic turnover of the Ti compound and b) operation in air rather than pure nitrogen gas.[51] The authors generated sodium naphthalenide in situ and then added $Ti(O^iPr)_4$ in ethereal solvent under nitrogen (Fig. 1.5). By addition of isopropyl alcohol (IPA) to release ammonia, with subsequent addition of sodium to regenerate the active reductant, they were able to achieve up to 340% yield vs Ti. Even more impressively, they were able to run this reaction under air, observing up to 44% yield vs Ti.

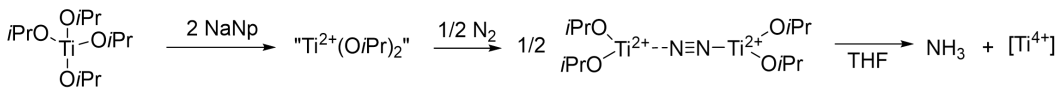

Figure 1.5: Catalytic titanium-mediated nitrogen reduction system by Van Tamelen and coworkers.[51]

Next, Van Tamelen and co-workers turned their attention to electrochemical Ti-mediated ammonia synthesis. In the first instance, 90 V was applied across two Pt electrodes in a solution of $Ti(O^iPr)_4$ and aluminum chloride ($AlCl_3$) in dimethoxyethane (DME) for two days under nitrogen.[52] Extreme conditions notwithstanding, they were able to achieve up to 10% yield of ammonia vs Ti (Fig. 1.6a). In keeping with prior observation, they also noted that ammonia formation did not begin until at least two equivalents of electrons had been passed per Ti compound. They also observed that the reaction turned blue while current was being passed up until one electron per Ti (which they hypothesized suggested the presence of Ti(III)), and then black (which they identified as a marker of a Ti(II) compound).

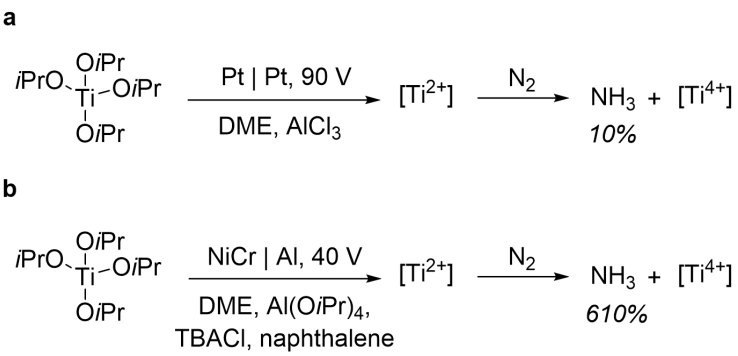

Figure 1.6: Electrolytic titanium-mediated nitrogen reduction system by Van Tamelen and coworkers.
a) Electrochemical TiNRR utilizing Pt electrodes.[52] b) Electrochemical TiNRR utilizing a NiCr cathode and an Al anode.[53]

Electrochemical TiNRR was then demonstrated catalytically as well.[53] A solution of $Ti(O^iPr)_4$, naphthalene, tetrabutylammonium chloride (TBACl), and aluminum isopropoxide ($Al(O^iPr)_3$) in DME under nitrogen was subjected to a 40-V electrolysis for 11 days. Again, these extreme conditions gave promising results: upon quenching, they measured 610% yield vs. Ti (Fig. 1.6b). They hypothesized that reduced nitrogen on Ti could be transferred to $Al(O^iPr)_3$, freeing the reduced Ti to fix more nitrogen and the reduced nitrogen to form ammonia. To test this hypothesis, they also introduced $Al(O^iPr)_3$ to the previously reported nitrogen reduction by NaNp and Ti.[51] Upon doing so, they were able to obtain a yield of 275% vs. Ti, suggesting that the Al center does indeed play a role in turning over the Ti complex.

At this time, Van Tamelen and co-workers performed several other crucial mechanistic studies. Their first important conclusion was that, indeed, ethereal solvent can act as a proton source in this reaction. They performed an experiment with potassium

metal, a titanium alkoxide, and nitrogen in deuterated THF and were able to measure 10% yield vs. Ti of deuterated ammonia in an acid trap.[56] Given the well-known propensity of ammonia to perform hydrogen-exchange in water,[59] the observation of any deuterated ammonia is an affirmative sign that the proton source is indeed the solvent. They also observed a significant KIE , with significantly more sluggish kinetics observed in deuterated THF. This suggested that, at least at ambient conditions, ammonia protonation is part of the rate-determining step.

The final mechanistic hypothesis made as part of this body of work was the suggestion that the active titanium complex is highly unstable and likely oligomerizes in the absence of nitrogen to form a less reactive Ti oligomer, which only slowly releases the active Ti complex. This hypothesis is supported by the evidence that the reaction happens much faster when titanium is reduced under nitrogen than when it is reduced under argon and subsequently exposed to nitrogen.[55] Hearkening back to Brintzinger's early EPR characterization of this system, the authors proposed that Brintzinger's hydrogen abstraction mechanism was likely a minor—possibly parasitic—pathyway.[42]

Finally, no accounting of titanium-mediated ammonia synthesis would be complete without a mention of the excellent work of Liddle and co-workers. There have been numerous reports of nitrogen binding and reduction from the 1970s up until the present day,[60–72] but Liddle was the first and only author since Van Tamelen to successfully demonstrate catalytic titanium-mediated ammonia synthesis.[73] The researchers utilized a triamidoamine-ligated titanium(III) complex with KC_8 reductant and trialkylphosphonium acid salts as proton source to generate ammonia with TON of the titanium complex up to 18 (Fig. 1.7): a record number in the field. They were able to obtain crystal structures of several of the key intermediates, finding an end-on-bound dinitrogen dititanium(III) dimer followed by a K^+-stabilized reduced nitrogen dititanium(IV) structure, which then rapidly underwent further reduction and protonation to release ammonia.

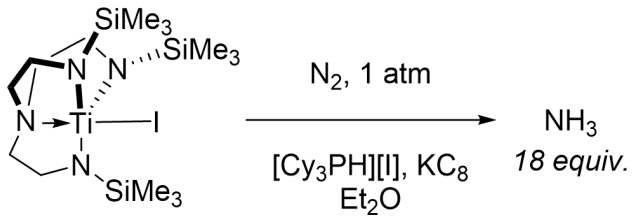

Figure 1.7: Catalytic titanium-mediated nitrogen reduction system by Liddle and coworkers.[73]

1.4 Thesis Outline

In this introduction, the history and background of artificial ammonia synthesis—in particular, the workings of the Haber-Bosch process, recent progress made in the field of LiNRR, and our accumulated knowledge of TiNRR—is discussed. Chapter 2 takes this background forward into the development of electrochemical TiNRR by replacing the thermochemical reductants used in the previously-outlined literature with an electrochemically-generated reductant—sodium naphthalenide—which can then reduce Ti. We find FEs of up to 24% and rates comparable to the highest rates reported in LiNRR, and discover that the rate-limiting step of this reaction is sodium plating.

In Chapter 3, this concept is taken a step forward and the sodium naphthalenide reductant is replaced with electrochemically-generated potassium metal. This reaction is significantly more selective—FEs above 50% are achieved—and displays moderate selectivity at ambient pressure. This is a significant advantage compared to the sodium naphthalenide system, which performs best at pressures of 10 bar nitrogen or above. A shift in the rate-determining step is observed in these two regimes. At high pressure, potassium plating is the rate-determining step, while at ambient pressure, the rate-determining step involves all three reaction components.

In Chapter 4, efforts are made at determining the mechanism of the reaction and expanding its scope. In situ UV-vis spectroscopy is attempted to identify discrete processes, and it is found that multiple processes are occurring at once, rendering the method limited in usefulness. A more detailed kinetic analysis is performed on the kinetic data presented in Chapter 3, resulting in a more detailed mechanistic proposal. Then, the hypothesis that potassium-titanium-mediated nitrogen reduction occurs in a stepwise electrochemical-thermochemical fashion is tested, and we find that, indeed, electrochemical potassium plating and thermochemical titanium and nitrogen reduction occur independently of each other. A study of the effect of proton donors on TiNRR is performed, in which it is discovered that—surprisingly—addition of proton donor does not have a pronounced effect on selectivity below a certain "tipping point" concentration. Finally, the scope of the reaction is expanded to different alkali metals and early transition metals.

Chapter 5 summarizes the research presented in this thesis and discusses how it can be used to further the field of electrochemical TiNRR and eventually decarbonize ammonia production.

Chapter 2

SODIUM-MEDIATED REDOX CASCADE FOR ELECTROCHEMICAL AMMONIA SYNTHESIS

(1) Klein, C. K.; Lindenfelser, A.; Yusov, M. A.; Jain, A.; Jones, R. J. R.; Gregoire, J.; Manthiram, K. *Joule* **2025**, *9*, 101923,

2.1 Abstract

Artificial ammonia synthesis is vital to modern life; however, the Haber-Bosch process, by which most ammonia is synthesized, is capital and carbon intensive. Zero-valent-metal-mediated ammonia synthesis is a promising alternative but requires a metal that is both a strong reductant and forms a stable nitride. Only a small number of metals, like lithium, can satisfy these constraints. Therefore, we developed an electrochemical paradigm enabling the use of different reductants by orthogonalizing the roles of the zero-valent metal between sodium metal and a Ti active site. These components are cheaper than lithium by two orders of magnitude. Using a sodium-naphthalene-titanium cascade, we achieved a rate of 475 nmol cm^{-2} s^{-1} and a faradaic efficiency of 24% and found that the reaction rate depends primarily on current density.

2.2 Introduction

Life on Earth as we know it could not be sustained without artificial ammonia synthesis. Ammonia is an essential component of fertilizers, and the ammonia produced from nitrogen and hydrogen in the Haber–Bosch process enables the world to support nearly double the population it could otherwise.[1] However, this process comes with costly downsides. It requires high temperatures (350-450 °C) and extreme pressures (150-200 bar), necessitating capital-intensive plants and around-the-clock, continuous operation. This precludes the use of most renewable energy sources, which are intermittent.[74] Additionally, ammonia synthesis is responsible for 1-2% of global CO_2 emissions and consumes 3-5% of the world's natural gas.[75] Such a paradigm is entirely incompatible with a clean energy future. Thus, it is vital to develop an alternative that can operate at milder conditions, make use of renewable energy sources, and reduce the CO_2 footprint.

Many such alternatives have been put forward, most of which rely on voltage to

drive the reaction rather than pressure and temperature.[76] Both heterogeneous and homogeneous methods of the electrochemical nitrogen reduction reaction (eNRR) have been successfully demonstrated.[77] The most reliable heterogeneous method of eNRR is the Li-mediated nitrogen reduction reaction (LiNRR)[25] which has demonstrated some of the highest partial current densities towards ammonia to date.[76] LiNRR is mechanistically quite simple (Fig. 2.1a). The electrolyte consists of nitrogen-saturated ethereal solvent, in which a lithium salt and a proton source are dissolved. Upon application of a reductive current at the cathode, lithium plates out to form Li^0, which reacts with nitrogen to form lithium nitride. This then reacts with the proton source in solution to produce ammonia and a Li(I) salt, which can theoretically be re-plated.[24]

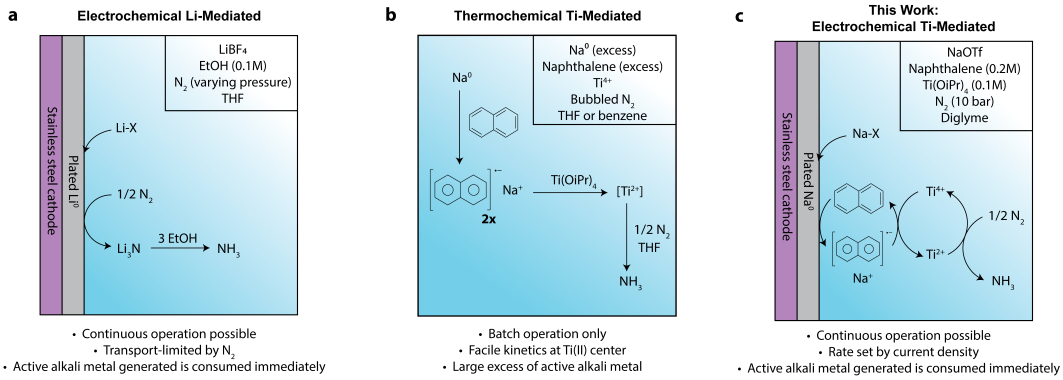

Figure 2.1: Schematic comparison of LiNRR and thermochemical Ti-mediated NRR to the proposed work.
a) Schematic of LiNRR. X = some counteranion (usually BF_4). b) Schematic of thermochemical TiNRR. c) Schematic of the sodium-mediated electrochemical cascade for eNRR described in this work.

Despite its high performance, LiNRR has several significant downsides. First, the combined function of reductant, nitrogen fixation center, and supporting electrolyte in a single species leaves little room for optimization. Additionally, the process uses expensive Li salts. These salts are two to three orders of magnitude more expensive than most other alkali metal salts, in part due to the burgeoning demand for lithium-ion batteries.[38,78] Cheaper metals have been pursued for this process: indeed, calcium and magnesium have recently been demonstrated to be capable of eNRR,[36,79] as these metals can spontaneously form a metal nitride like lithium. However, the list of metals that are productive for eNRR is limited: the plated metal must spontaneously form a metal nitride under ambient conditions, but the nitride cannot be too stable, or the protonation step becomes difficult.[80] Additionally, the key nitridation step is often slow, limiting the overall rate of reaction in non-Li eNRR systems.

Therefore, it would be ideal to develop a system in which the compounds involved in the electrochemical and thermochemical steps are orthogonalized, without sacrificing the kinetic facileness of nitrogen reduction in the presence of an alkali metal reductant.

To address these challenges, we developed a strategy to decouple the electrochemical and thermochemical steps, enabling greater control over each process while maintaining the kinetic advantages of nitrogen reduction in the presence of an alkali metal reductant. We sought a reductant that is cheaper and has a more positive reduction potential than lithium and a nitrogen-binding site that can achieve high rates of thermochemical nitrogen fixation. Successful NRR has been demonstrated thermochemically via reduction with sodium naphthalenide of Ti(IV) to Ti(II), which is capable of reducing N_2 under even ambient conditions[54,55] (Fig. 2.1b). Based on these studies, we utilized an electrolyte containing a Na(I) salt, naphthalene, and titanium tetraisopropoxide ($Ti(O^iPr)_4$) in diglyme at 10 bar N_2 pressure to accomplish our goal (Fig. 2.1c). In this cascade system, nitrogen reduction is enabled by first plating sodium, the key electrochemical step, followed by reduction of naphthalene to sodium naphthalenide (NaNp) and subsequent reduction of Ti(IV) to Ti(II), which binds to N_2 and splits the triple bond. In contrast to LiNRR, in this system, the species that is electrochemically reduced (i.e., Na^+) is different from that which binds and reduces nitrogen (i.e., the titanium complex). Hence, the interfacial electron transfer and nitrogen bond scission steps can be tuned independently of each other. Under our conditions, we have achieved rates of NH_3 production up to 475 nmol cm^{-2} s^{-1} and 24% faradaic efficiency (FE), comparable to the rates achieved by many state-of-the-art LiNRR systems.[26,27,81] We also find that under our most optimized conditions, the rate of reaction in this cascade depends *only* on the rate of sodium plating, providing a path for further improvement of rate and selectivity.

2.3 Results

Electrochemical proof of concept validated

A series of studies from van Temelen and coworkers in the late 1960s[54–56] demonstrated the use of a Ti(II) intermediate, formed in situ with the help of an alkali metal reductant, to reduce nitrogen to ammonia. It is generally postulated that it is the Ti(II) species which binds N_2 and performs the first electron transfer, but that subsequent reduction steps may be assisted by the active reductant.[82] We identified a model thermochemical system consisting of $Ti(O^iPr)_4$, NaNp (generated in situ from Na(0) and naphthalene) as the reductant, and THF as the solvent.[56] These were cho-

sen on the basis of simplicity, low reagent cost, and good thermochemical yield on a reasonable reaction timescale. Many systems based on Ti(II) complexes operate on a timescale of days to weeks;[46] in the model thermochemical system, when the reagents specified above were combined at ambient conditions, we were able to obtain 25% ammonia yield vs. Ti in 5 hours at a rate of 1 nmol s^{-1}. This result is comparable to that obtained in the original studies.[56]

We sought to electrify this reaction, replacing the stoichiometric NaNp used in the thermochemical model system with a suitable sodium salt and naphthalene. Our design principles were (1) solubility of all components in a single solvent; (2) conductivity of the electrolyte solution to allow for a reasonable overall cell potential (i.e. one that would not overload a standard Biologic potentiostat); (3) safety of all components and byproducts. The third design principle ruled out the common sodium-ion battery salts $NaClO_4$, which is shock-sensitive when dry, and $NaPF_6$, which dissociates easily to form HF and NaF in the presence of water. Initial optimization (Figs. S2.1–S2.2) led us to identify 1 M sodium triflate (NaOTf) in diglyme with 0.2 M naphthalene and 0.1 M $Ti(O^iPr)_4$ as fulfilling all three requirements. At a current density of -54 mA cm^{-2} with a stainless steel working electrode and a Pt counter electrode, we were able to achieve FEs of up to 18.6% in this sodium-naphthalene-Ti-mediated eNRR (NaNpTiNRR) cascade. Cyclic voltammetry (CV) of the system confirmed that the only fully electrochemical step was Na plating. The CV of the electrolyte solution showed a Na plating and stripping peak in the absence of Ti and naphthalene. However, in the presence of all reagents, only a plating peak was observed, suggesting that the plated Na is reacting with other components of the electrolyte (Fig. 2.2a).

Control experiments demonstrate robust electrochemical ammonia synthesis

Due to the preponderance of false positives in the field of NRR, we performed a series of experiments to validate both the source of ammonia as N_2 and the necessity of all reactants for reduction to proceed. We found that in the absence of NaOTf, $Ti(O^iPr)_4$, N_2, or current, the reaction did not proceed (Fig. 2.2b). However, in the absence of naphthalene, the reaction proceeded—albeit much less selectively—suggesting an alternative reduction pathway wherein plated sodium metal directly reduces Ti, rather than first forming sodium naphthalenide.

NH_3 was primarily quantified via the salicylate assay. However, given the known sensitivity of the salicylate assay to trace metals,[83] we also independently performed

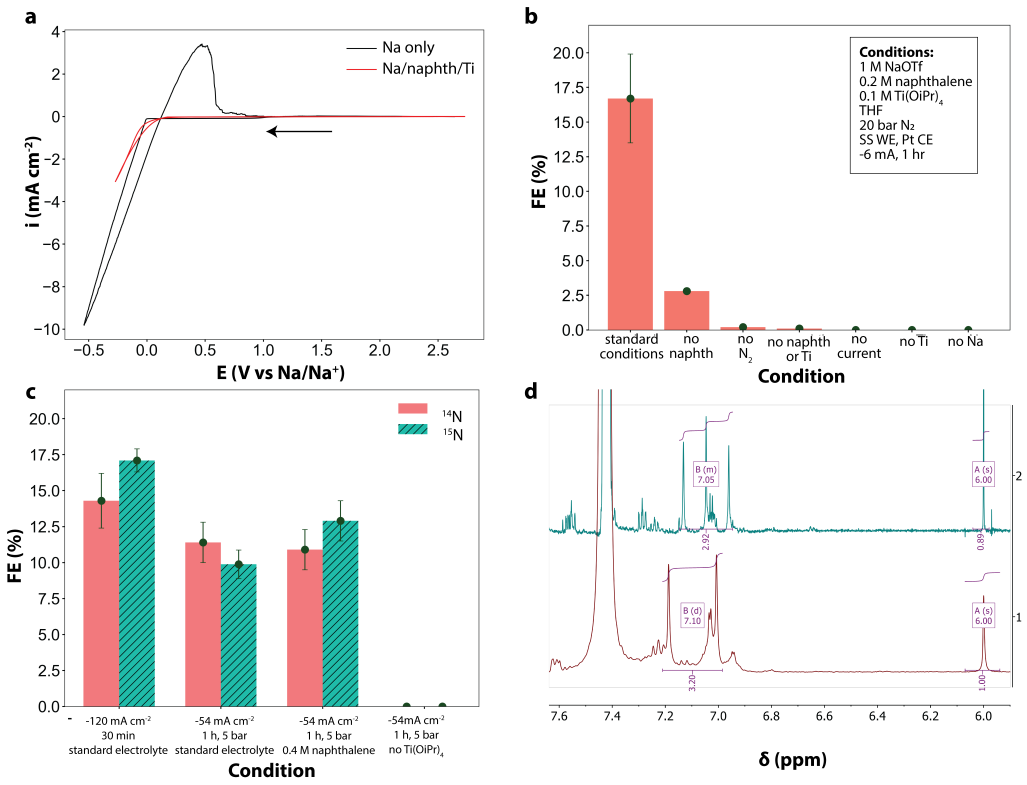

Figure 2.2: Initial proof-of-concept results and controls.

Raw data for (B) and (C) can be found in Table S2.1, and an expanded view of the NMR spectra in (D) is shown in Figures S2.5 and S2.6. Representative chronopotentiograms of the standard conditions and no-Ti controls are shown in Figs. S2.7 and S2.8.

a) CVs of the electrolyte solution with and without naphthalene and Ti. 1 M NaOTf, 0.1 M $Ti(O^iPr)_4$, 0.2 M naphthalene, and diglyme; stainless steel working electrode (area = 0.1017 cm^2), Pt counter electrode, and Pt pseudo-reference; and scan rate 20 mV/s. E: potential at the working electrode; i: measured current density.

b) Control studies of the electrochemical reaction in the absence of each of the reagents. Error bars represent the standard deviation between replicates of the same experiment. All experiments were run at least in duplicate.

c) Plot of FEs measured in experiments using $^{14}N_2$ vs. $^{15}N_2$ as feedstock. The "standard electrolyte" referred to in the figure is 1 M NaOTf, 0.1 M $Ti(O^iPr)_4$, 0.2 M naphthalene, and diglyme; stainless steel working electrode (area = 0.1017 cm^2) and Pt counter electrode. The "0.4 M naphthalene" condition used 0.4 M naphthalene rather than 0.2 M naphthalene but was otherwise identical. The "no Ti" condition used the same standard electrolyte but with no $Ti(O^iPr)_4$ added. Error bars represent either the standard deviation between replicates of the same experiment (^{14}N experiments) or the uncertainty in quantification (^{15}N experiments). All ^{14}N experiments were run at in duplicate; ^{15}N experiments were run in singlicate.

d) ^1H NMR of a ^{15}N isotope labeling control (NMR solvent DMSO-D_6), showing the characteristic doublet of $^{15}NH_4^+$ as well as the internal standard, 1,3,5-trimethoxybenzene (TMB), as a singlet at 6.0 ppm.

replicates and quantified them by ^{1}H NMR, which gave nearly identical results (Figs. S2.3–S2.4). We also confirmed that the ammonia formed was from the nitrogen feed gas and not from spurious sources by performing replicates of select points with $^{15}N_2$ gas (Fig. 2.2c). If $^{14}NH_4^+$ was formed, it was present in levels below the detection limit of NMR. This can be seen in Fig. 2.2d, which shows a clear doublet (corresponding to $^{15}NH_4^+$) and no triplet (which would correspond to $^{14}NH_4^+$). The FEs measured from experiments using $^{15}N_2$ as a feedstock match very closely with the corresponding $^{14}N_2$ experiments, and no ammonia was observed with either gas when $Ti(O^iPr)_4$ was omitted from the electrolyte.

Mechanistic investigation reveals rate depends only on current density

In LiNRR, increasing nitrogen pressure is a common strategy to overcome transport limitations and to have lithium nitridation (productive path towards ammonia) outcompete lithium protolysis (undesired path towards hydrogen). Thus, we investigated the pressure dependence of the NaNpTiNRR cascade. For this system too, we expected the reaction to be kinetically limited by nitrogen at atmospheric pressure, especially since the rate of the thermochemical Ti(II) catalyzed reaction at atmospheric pressure is slow.[56] Indeed, this was the case; at pressures below 10 bar, the reaction is limited in nitrogen. However, at and above 10 bar, the reaction rate no longer depends on N_2 partial pressure (Fig. 2.3a). Therefore, all subsequent reactions were performed at 10 bar N_2 pressure. While the system exhibits saturation kinetics in nitrogen, we observed zero-order dependence on both naphthalene (Fig. 2.3b) and titanium (Fig. 2.3c) concentrations.

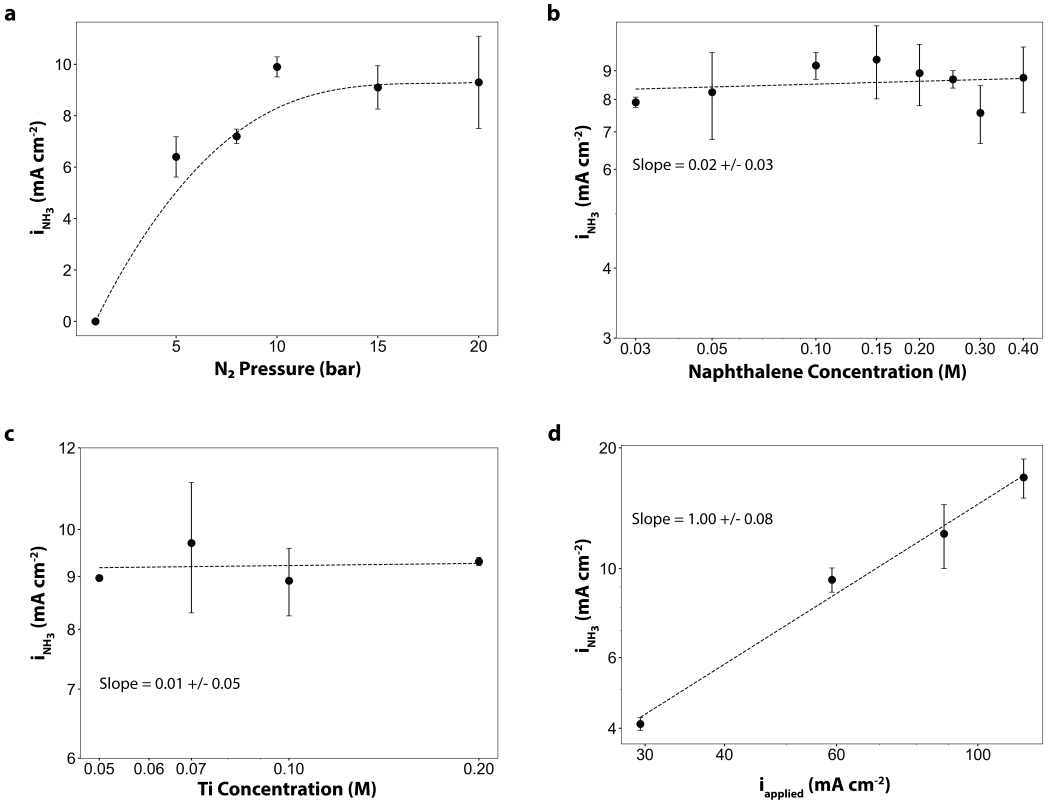

Figure 2.3: Optimization of the sodium-mediated redox cascade for nitrogen reduction.

Except where otherwise specified, all reactions were performed in an electrolyte consisting of 1 M NaOTf, 0.1 M $Ti(O^iPr)_4$, and 0.2 M naphthalene in diglyme at 10 bar N_2 pressure. -54 mA cm^{-2} was passed for 1 hour with a stainless steel working electrode and a Pt counter electrode. All labeled slopes are from log-log plots (i.e. the calculated slopes are equivalent to the rate orders); the data is plotted on log scale.

a) Plot of current density towards ammonia at varied N_2 pressures, with a Bézier fit to illustrate the shape of the isotherm.

b) Plot of partial current towards ammonia at varied naphthalene concentration; all measurements were taken at a Ti concentration of 0.1 M.

c) Plot of partial current towards ammonia at varied $Ti(O^iPr)_4$ concentrations; all measurements were taken at a naphthalene concentration of 0.2 M.

d) Plot of partial current towards ammonia at various applied current densities.

2.4 Discussion

At the optimal operating conditions, the rates of nitrogen fixation to ammonia are insensitive to nitrogen partial pressure, naphthalene concentration, and Ti concentration. Thus, the rate-limiting step must be early in the reaction cycle, before these species are involved. By examining a hypothesized mechanism based on the thermochemical Ti(II)-based nitrogen fixation literature and our results (Fig. 2.3a), the only candidate step that satisfies this constraint is sodium plating. We would thus expect the rate to scale linearly with applied current density, since generation of zero-valent sodium is coulometrically controlled. In agreement with this, we find a first-order dependence on current density (Fig. 2.3d). Promisingly, this means that all subsequent thermochemical steps are significantly faster than sodium plating, and that the reaction could be further optimized by tuning the solid electrolyte interphase structure formed by sodium metal.[84] We tested the extent of this dependence by applying a current density of -688 mA cm^{-2} (the highest current density we could apply given the voltage limits of the potentiostat) over 10 minutes. As expected, this yielded a FE of 24%, and a rate of 475 nmol cm^{-2} s^{-1}, a rate higher than nearly all published LiNRR systems.[26,27] Indeed, if rate is calculated on the basis of electrochemical rather than geometric surface area, this is the highest reported rate in a LiNRR-type system.[27] This demonstrates the high utility of a system whose rate is controlled entirely by current density over an extremely wide range of currents.

These discoveries are mechanistically significant, as the rate and order dependence of this electrochemical reaction are very different from the corresponding thermochemical reaction. These mechanistic discoveries have practical implications as well. Most importantly, the invariance of rate on concentration and pressure at the ideal operating conditions makes the cascade system robust and resilient to perturbations. This means that ammonia can be continuously produced at a constant rate even if there are transient variations in conditions such as pressure or mediator concentration.

This postulated catalytic cycle, while useful for identifying a possible rate-determining step, does not address all mechanistic questions. Aspects of this cycle that are still in doubt are: (1) the identity of the proton source, shown in Fig. 2.4a as A-H (see Supplementary Note 2.1 for a brief discussion of the effect of water on this system); (2) the oxidation state of the active Ti center, hypothesized here to be Ti(II); (3) whether or not it is truly a cycle, i.e., whether or not a turnover number (TON) > 1 can be achieved for Ti. These questions have all been answered in the thermochemical case.

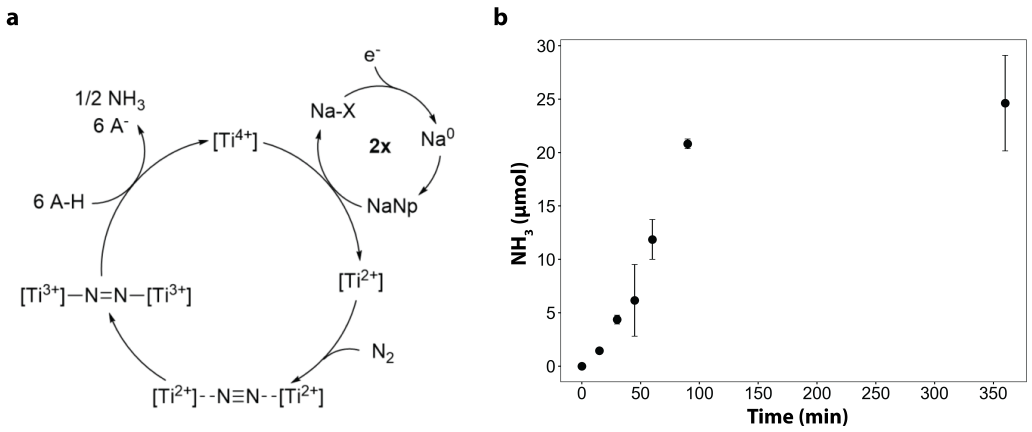

Figure 2.4: Postulated mechanism of NaNpTiNRR and plot of µmols of ammonia formed vs. time.

a) Postulated mechanism of NaNpTiNRR; A-H indicates a generalized proton source, most likely the ethereal solvent.

b) Plot of µmols of ammonia formed vs. time; the reaction was performed in an electrolyte consisting of 1 M NaOTf, 0.1 M $Ti(O^iPr)_4$, and 0.2 M naphthalene in diglyme at 10 bar N_2 pressure. A constant current of -54 mA cm^{-2} was passed with a stainless steel working electrode and a Pt counter electrode.

Van Tamelen and colleagues demonstrated that the ethereal solvent is the proton source using deuterium isotope labeling;[56] they showed that the Ti complex must be reduced with at least two electrons before any nitrogen reduction begins, suggesting that the active Ti center is reduced to at least the 2^+ state;[52] and they achieved TON > 3 under conditions that were, unfortunately, never fully disclosed.[51] While (1) and (2) are questions beyond the scope of this study, we attempted to achieve a Ti TON >1 by running our standard conditions at longer times. However, after 2 h of reaction time (equivalent to 43.2 C passed), the amount of ammonia in the cell stayed constant (Fig. 2.4a). We were able to rule out the possibility of significant ammonia oxidation at the anode (see Supplementary Note 2.2 for details), suggesting that the Ti compound does deactivate at this point. This could be due to complexation of the Ti compound with H_2, which is likely formed at the cathode as a parasitic side product, or with anode oxidation byproducts. These problems could be addressed by further improvement of catalyst selectivity or with reactor engineering.

These unresolved aspects, while challenging, present exciting opportunities for further investigation in our electrochemical system. Strategies utilized to great effect in the LiNRR literature would likely be applicable in optimizing this reaction as well. For instance, one possible method of making the reaction continuous would involve incorporation of both a separator and a stable proton shuttle into the system—for

instance, the phosphonium ylide used to striking effect by MacFarlane and coworkers[32]—and then utilizing hydrogen oxidation at the anode as the terminal proton source.[33] This could be used in combination with a recirculating electrolyte—as demonstrated recently by Chorkendorff and coworkers[81]—to further stabilize the solution and allow turnover of the Ti compound, as well as increase the energy efficiency of the system (see Supplementary Note 2.3).

This study has put forth an alternate method for synthesizing ammonia, with rates and current densities that outcompete all but one LiNRR system,[27] vastly outperform the rates of comparable thermochemical systems, and utilize reagents that are several orders of magnitude cheaper. Excitingly, this cascade system offers the possibility of orthogonalizing the roles of shuttling electrons, done via a plated alkali metal and naphthalene, and nitrogen fixation. We anticipate that the ability to apply the strong reducing power of zero-valent alkali metals to homogeneous systems electrochemically will be of use in developing developing diverse electrosynthetic reactions, and ultimately contribute towards decarbonizing chemical synthesis.

2.5 Experimental

Materials

Tetrahydrofuran (THF, anhydrous, 99.5%, stabilized with BHT), diglyme (DG, anhydrous, 99.5%), sodium triflate (NaOTf, 98%), naphthalene (suitable for scintillation, ≥99%), titanium tetraisopropoxide ($Ti(O^iPr)_4$, 97+%), sodium salicylate (ReagentPlus®, ≥99.5%), sodium nitroprusside (99+%), and mol sieves (3 Å, 4-8mesh) were purchased from Sigma-Aldrich. Sodium hypochlorite (NaOCl, 10-15%) was purchased from VWR International. Milli-Q water was obtained by filtering deionized (DI) water through a Milli-Q purification system (Merck, Millipore Corporation). Deuterated dimethylsulfoxide ($DMSO\text{-}D_6$) was purchased from Alfa Aesar. Nitrogen gas (UHP, 99.999% purity) and argon gas (UHP, 99.999% purity) were purchased from Airgas. Platinum foil (0.1 mm thick, 99.99% trace metals basis) was purchased from Beantown Chemical. Stainless steel wire (0.025 gauge, Malin Co.) was purchased from McMaster-Carr.

Methods

Electrolyte solution preparation

Dry DG was used as the solvent in DG-based experiments described below. It was obtained by drying as-purchased anhydrous DG over 20% v/v of freshly dried molec-

ular sieves for at least 48 hours in an Ar-filled glovebox. The sieves were prepared by washing with acetone and then drying at 400 °C for at least 4 hours in a muffle furnace. They were pumped directly into an Ar-filled glovebox and stored there before use. Dried NaOTf, as-purchased naphthalene, and as-purchased $Ti(O^iPr)_4$, all stored in an Ar glovebox, were dissolved in DG to obtain electrolyte solutions of varying concentrations. NaOTf was dried overnight in a vacuum oven at 90 °C before being brought into the glovebox. The resulting cloudy-white electrolyte solution was brought out of the glovebox and centrifuged at 3400 rpm for 10 minutes to remove insoluble residue. The resulting clear supernatant was transferred to an oven-dried vial through which nitrogen was bubbling at 20 sccm and nitrogen was bubbled through it for at least 10 minutes to saturate the solution. The electrolyte could be stored in the glovebox for up to a week without any noticeable change in faradaic efficiency; however, once it was removed from the glovebox, it was used within 1-2 hours maximum.

Thermochemical nitrogen reduction experiments

In a typical thermochemical nitrogen reduction experiment, sodium metal (276 mg, 12 mmol) and naphthalene (1.6 g, 12.2 mmol) were mixed in 20 mL dry THF in an Ar-filled glovebox, forming a green solution. $Ti(O^iPr)_4$ (2 mmol, 568 mg) was added, forming a black solution. This was then brought out of the glovebox and N_2 was bubbled through the solution for 5 hours. The reaction was quenched by dropwise addition of 20 mL water, forming a grey precipitate. This was removed by centrifugation at 3400 rpm for 10 min. The resulting clear supernatant was diluted to 100 mL total in a volumetric flask and quantified using the salicylate method (described below).

Conductivity measurements

The conductivity measurements shown in Fig. S2.1 were performed on a Hanna HI5521 benchtop combination pH and resistivity meter. 10 mL of the electrolyte tested were prepped in the glovebox, then taken out and tested on the bench.

Electrochemical nitrogen reduction experiments

High-pressure nitrogen reduction experiments were performed using cells machined out of PEEK and stainless steel (Figs. S2.9–S2.10). The cells were oven-dried at 105 °C for at least 20 minutes before use. They were assembled while still hot and then

dry nitrogen was blown through them to cool them down without allowing water to condense. Electrolyte was not added until the cells were at room temperature.

The counter electrode was a 25x25 mm Pt foil, placed on top of a stainless steel current collector. The working electrode was a stainless steel 0.025 gauge wire. The wire was pushed through a length of PEEK tubing (1/16" OD, 0.03" ID) such that it was exposed on both ends. One end was chosen to be the working electrode and was measured with a caliper to be exactly 5.2 mm tall (resulting in a total area of 0.107 cm^2). The other end was epoxied to the PEEK tubing to create a pressure-tight seal. No reference electrode was used in standard electrochemical experiments; when a reference was required (for example, in the CVs in Fig. 2.2a of the manuscript), a pseudo-reference electrode was used, consisting of a Pt wire fashioned in the same way as the stainless steel working electrodes. Due to significant reference drift, we chose not to use an internal standard for calibration and simply set the zero point to be the Na plating potential observed.

1.7 mL of nitrogen-saturated electrolyte was added to the pressure cell under active N_2 flow. The working electrode was screwed in to seal the pressure cell and the cell was pressurized to the chosen pressure (usually 10 bar). A chosen constant current was applied using a Biologic VMP3 potentiostat. In a typical experiment, 21.6 C were applied.

Upon completion of the experiment, the cell was depressurized and the electrolyte removed. In any successful experiment with Ti present, the electrolyte turned black. It was diluted in water, upon which it turned a pinkish-brown color. The interior of the pressure cell was then rinsed with water three times and added to the sample as well, and diluted to roughly 13 mL in a 15 mL Falcon tube.

The diluted sample was then centrifuged for 10 minutes at 3400 rpm and the resulting clear supernatant was added to a 100 mL volumetric flask and diluted to the mark. Two samples for ammonia quantification were made: one usually diluted 2X and one diluted 4X. All cells were run in duplicate. They were quantified using the salicylate method (described below).

All cell parts, the Pt counter electrode, and the current collector were sonicated successively in acetone and water, rinsing with water in between. The working electrode was rinsed with acetone and water. The Pt counter electrode was washed and reused; the working electrode was replaced each time. After washing, all cell parts were dried under a stream of nitrogen and placed in an oven at 105 °C for at least 20

minutes before use.

Ammonia quantification – salicylate method

Ammonia was quantified using the salicylate method, which has been described in detail elsewhere.[24] In brief: 2 mL of sample was prepared, diluted to an appropriate concentration such that the resultant UV-Vis absorption was not expected to exceed 1.0. To this was added 280 µL of an aqueous salicylate solution (consisting of 2.5 M sodium salicylic acid and 0.5 mM sodium nitroprusside, stored at 4 °C in the dark for up to three months) and 280 µL of an alkaline solution (made just beforehand by mixing 10-15% NaOCl and 0.4 M aq. NaOH in a 1:9 volume ratio), mixed thoroughly, and allowed to develop in the dark at room temperature for 1.5 hours, resulting in a blue color if ammonia was present. The solution absorbance spectrum was then measured with an Agilent Cary 60 UV-Vis spectrophotometer. The relevant absorption peak was taken to be the difference between absorbance at 650 nm and 475 nm.

Aqueous calibration curves were used to calculate the resulting concentration of ammonia in solution. They were made by preparing aqueous solutions of 0, 30, and 60 µM NH_4Cl, which were then measured in the exact same way as the experimental samples. Calibration curves were made fresh every week to ensure that there was no contamination in the water or reagents used for quantification.

Calculation of faradaic efficiency from salicylate assay

Faradaic efficiency was calculated from the concentration obtained from the calibration curve using the following equation:

$$FE_{NH_3} = \frac{C_{NH_3} \cdot V \cdot n \cdot F}{It}$$

where C_{NH_3} is the concentration of ammonia in the sample (M), V is the volume to which the electrolyte was diluted (usually 0.1 L), I is the current (usually 0.006 A), t is the total experiment time (usually 3 600 s), n is the number of electrons consumed per mole of ammonia produced (this number is always 3), and F is Faraday's constant (96 485 C mol e-1).

Ammonia quantification – NMR

Ammonia was quantified by NMR on a Bruker 400 MHz spectrometer with broadband iProbe using a method adapted from MacFarlane and coworkers.[85] The method of standard addition was used to quantify ammonia. The samples were prepared by mixing 300 μL of DMSO-D_2, 200 μL of used electrolyte, 50 μL of 4M aq. H_2SO_4, 50 μL of a stock solution of 14mM TMB in DMSO, and finally 100 μL of an aqueous solution of NH_4Cl for a total volume of 700 μL. For each cell quantified, five NMR samples were prepared in total: one with no added NH_4Cl, and then four with, sequentially, 250, 500, 750, and 1000 μM NH_4Cl.

NMR spectra were taken using a modified SELGPSE pulse with a relaxation delay of 10 seconds and 16 scans.

Calculation of faradaic efficiency from NMR assay

NMR spectra were processed using MestReNova; examples are shown in Figs. S2.5, S2.6, and S2.11. In brief: the peak of the internal standard TMB was integrated to 1, and the area of the peak corresponding to NH_4Cl was referenced accordingly and recorded. The NH_4Cl peaks overlapped significantly with naphthalene peaks, so MestReNova integral manager was used to deconvolute peaks and calculate the area of only those corresponding to ammonium. A plot was then constructed of peak area vs. concentration of the known standards and the linear fit extrapolated back to the x-axis, giving the concentration of NH_4Cl in the NMR sample. This number was then converted to FE by the following equation:

$$FE_{NH_3} = \frac{C_{NH_3} \cdot \frac{7}{2} \cdot 1.7 \cdot 10^{-9} \cdot n \cdot F}{It}$$

It is expected that this number will be slightly less accurate than the salicylate method, because the salicylate method is diluted to a known volume, while in this method the volume of electrolyte (1.7mL) is assumed.

Comparison of calculated FE from NMR and salicylate assays

The volume of one cell was not enough to run both NMR and salicylate assays on the same sample; therefore, we ran two identical cells (the electrolyte was 1M NaOTf, 0.2M naphthalene, 0.1M $Ti(O^iPr)_4$ in diglyme; a stainless steel cathode and Pt anode were used; -12mA were applied for 30 minutes under 10 bar N_2 pressure). Then one was quantified by the salicylate assay and the other by NMR. The two yields agreed

with each other within error (data shown in Figs. S2.3 and S2.4): by salicylate, the FE was 16.8%, and by NMR, it was 14.4%.

Procedure for $^{15}N_2$ controls

$^{15}N_2$ controls were performed in the same way as the standard method, with a few changes made to conserve expensive isotope-enriched nitrogen. The flow rate of $^{15}N_2$ used to purge the electrolyte was 10 sccm instead of 20, and the electrolyte was only purged for 8 minutes rather than 10. Additionally, the high-pressure cells were assembled, filled with the purged electrolyte, and directly pressurized rather than being flushed with nitrogen first. These changes likely resulted in a slight increase in the amount of adventitious water, oxygen, and other contaminants; however, they did not have any noticeable effect on yield. Example calibration curves for calculation of FEs in these experiments are shown in Figs. S2.12–S2.13.

2.6 Funding Acknowledgment

This research was supported by the National Science Foundation under grant 2204756. This material is based upon work supported by the National Science Foundation Graduate Research Fellowship under grant no. 2139433. The authors gratefully acknowledge the support of the Resnick Sustainability Institute.

The authors gratefully acknowledge the Dow Next Generation Fund, which donated the Bruker NEO 400 on which we collected all ^{1}H NMR spectra to the Caltech Liquid NMR Facility. We also thank Dr. David Vander Velde, manager of the Caltech Liquid NMR Facility, for his invaluable advice and help collecting and interpreting ^{1}H NMR spectra of ammonium ion in complex mixtures.

2.7 Supplementary Material

Supplementary Notes

Supplementary Note 2.1: Water Content

Because many of the active reagents in our reaction are water-sensitive, we measured the water content in a representative sample of electrolytes using a Karl-Fischer titrator. The electrolyte was then used in an electrochemical cell as usual and the associated FE was recorded (Fig. S2.14). As expected, a higher water content (260ppm corresponds to >10 mM water) decreased FE. However, in general, the day-to-day water content of electrolytes was very consistent.

Supplementary Note 2.2: Anode Controls

Since our cells were small and unseparated, it was important for us to determine to what extent anodic reactions might be interfering directly with ammonia yield. We were particularly concerned that our Pt anode might be oxidizing ammonia in situ. Therefore, we performed two controls: a spiked ammonia control and a no-Pt control.

The purpose of the spiked ammonia control was to determine whether the Pt anode would oxidize any ammonia under our usual conditions. To this end, an electrolyte was prepared in the usual way as described below, but Ti was removed and the electrolyte was spiked with 10 mM NH_4OTf. This concentration was chosen as it is in the range of concentrations seen in a typical NaNpTiNRR run. We then ran 2 experiments: one where we pressurized the electrolyte in the cell, but did not apply current, and the other where we pressurized and applied current. We then quantified ammonia using the salicylate assay as described below. We quantitatively recovered the ammonia spiked into the cell with no applied current; however, only 84% of the ammonia spiked into the cell with applied current was recovered. This suggests that some ammonia is being oxidized away, and that our reported yields may be lower than the "true" yields accessible without a Pt anode. However, the faradaic efficiency towards ammonia oxidation at the anode under these conditions is only 3%, so it is unlikely that ammonia oxidation is a dominant anodic process at any point in the reaction.

Supplementary Note 2.3: Energy Efficiency

Energy efficiency is an important metric which has been much discussed in the LiNRR literature[24,81] and which deserves addressing. However, a 1:1 comparison with LiNRR systems is difficult, for several reasons. The most important one is that the proton source in this system is not yet defined, while in LiNRR it has been well established that one can source protons from hydrogen oxidation occurring at the anode. Incorporation of hydrogen into our Ti system would be difficult as H_2 inhibits Ti reactivity.[82] However, we can calculate maximum energy efficiency in the ideal case by accounting for energy stored in chemical bonds as E_{out} relative to energy input via electricity as E_{in}:

$$EE_{max} = \frac{E_{out}}{E_{in}} = \frac{V^0_{NH_3}}{V^0_{Na}}$$

$V^0_{NH_3}$ is the thermodynamic cell potential for cathodically generating ammonia relative to water oxidation at an anode. V^0_{Na} is the thermodynamic cell potential for sodium plating relative to water oxidation.

Which, in the ideal case of 100% FE, perfect efficiency for hydrogen production relative to oxygen evolution, and no cell resistance, reduces to:

$$\frac{1.17}{1.23 + 2.71} = \frac{1.17}{3.94}$$

where 2.71 V is the standard reduction potential of sodium, giving a maximum possible energy efficiency of 29.7%, higher than the theoretical maximum for LiNRR2.

We can compare this ideal value to what we experimentally obtain in practice. The more straightforward approach in this instance is simply to convert the amount of ammonia produced to a theoretical energy (that produced by complete combustion of ammonia to water) by the following equation:

$$E_{out} = n_{NH_3}\Delta G^0_{R,NH3toH2O} = n_{NH3} * V^0_{NH3} * Z * F = 3 * F * n_{NH3} * 1.17 = FE * 1.17 * Q$$

where Q is total charge passed, $\Delta G^0_{R,NH3toH2O}$ is the Gibbs free energy of reaction for complete combustion of ammonia to water, nNH3 is the number of moles of NH3, Z is the charge (which in the case of NRR is always equal to 3), F is Faraday's constant, and FE is faradaic efficiency. Then, we can divide this energy by the total power input into the system, calculable by simply multiplying the cell voltage V by Q, to get an equation for actual electricity-to-ammonia energy efficiency (EE_{actual}).

$$EE_{actual} = \frac{1.17 * FE}{V}$$

Based on this equation, we calculate an energy efficiency for our standard cell of 2.0%.

Supplementary Figures

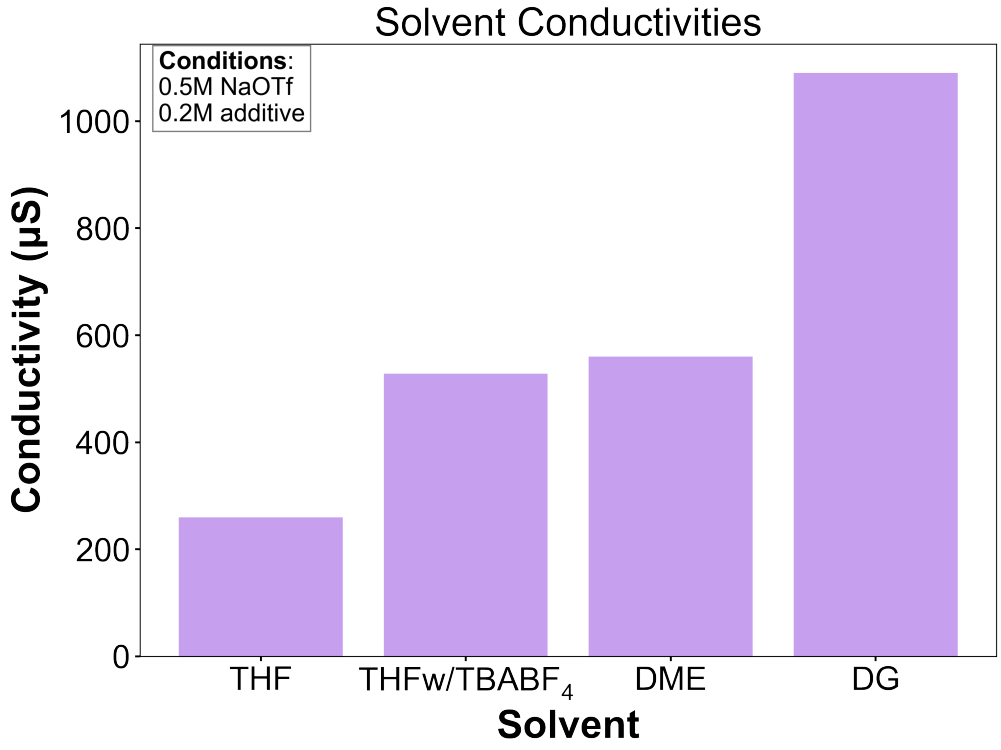

Figure S2.1: Comparison of conductivities of different electrolyte salt/solvent combinations.

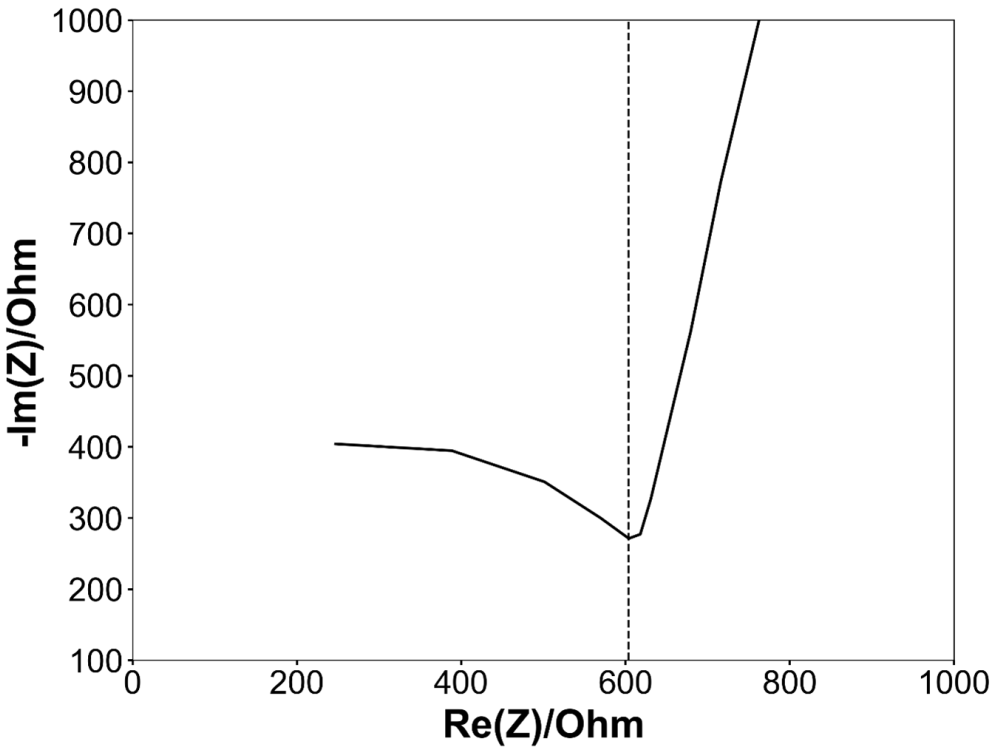

Figure S2.2: Plot of the real and imaginary components of resistivity as measured by potentiostatic electrochemical impedance spectroscopy (PEIS).
Electrolyte: 1M NaOTf, 0.3M naphthalene, 0.05M $Ti(O^iPr)_4$ in diglyme. Cell was pressurized to 10 bar N_2 and PEIS run from 200 kHz to 100 mHz at open circuit potential.

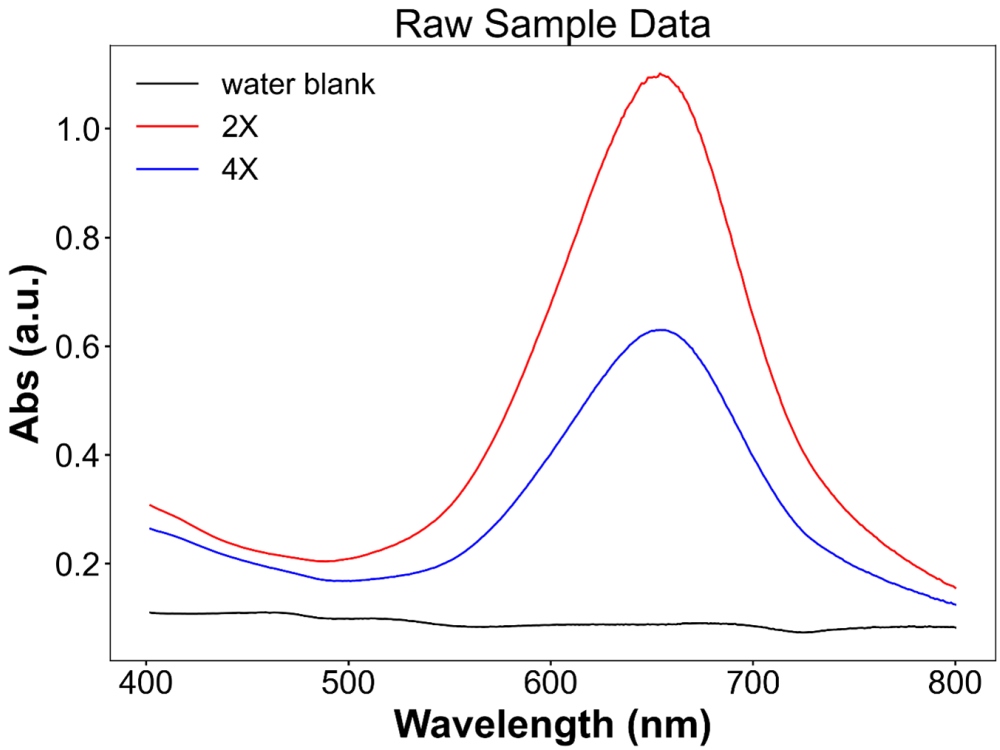

Figure S2.3: UV-vis plot of two dilutions of the same sample run on NMR. FE as calculated by this method: 16.8%.

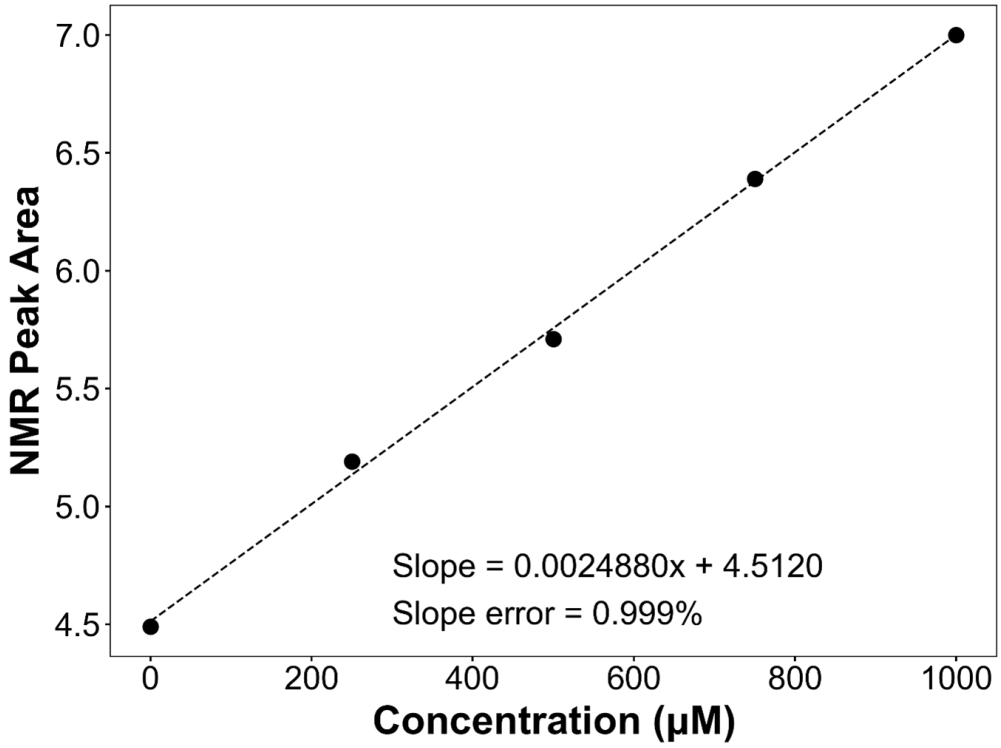

Figure S2.4: Plot of NMR peak area vs. $^{14}NH_4^+$ concentration (μM) used to determine the FE towards ammonia of a typical experiment using the method of standard addition.

Experimental conditions: 1M NaOTf, 0.2M naphthalene, 0.1M $Ti(O^iPr)_4$ in diglyme, stainless steel working electrode, Pt counter electrode. FE as calculated by this method: 14.4%.

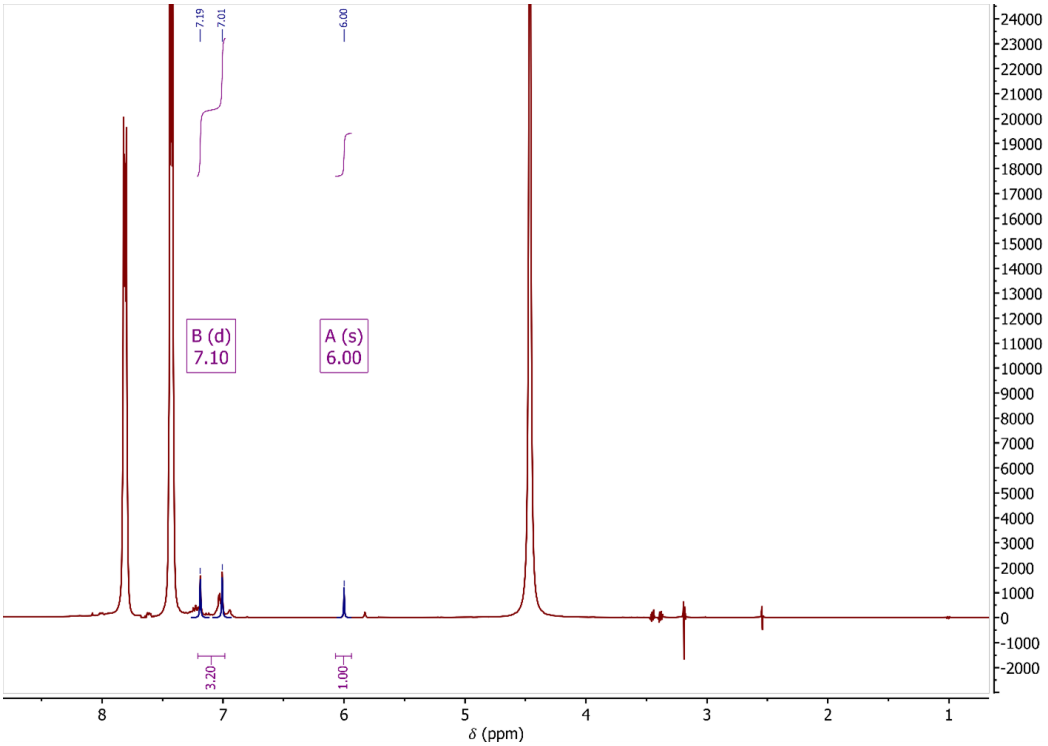

Figure S2.5: Sample spectrum of 1H NMR on an electrolyte sample containing $^{15}NH_4^+$.

The ammonium signal is a doublet at 7.10ppm, while the TMB used as a reference is a singlet at 6.00ppm. The NMR solvent is DMSO-D_6.

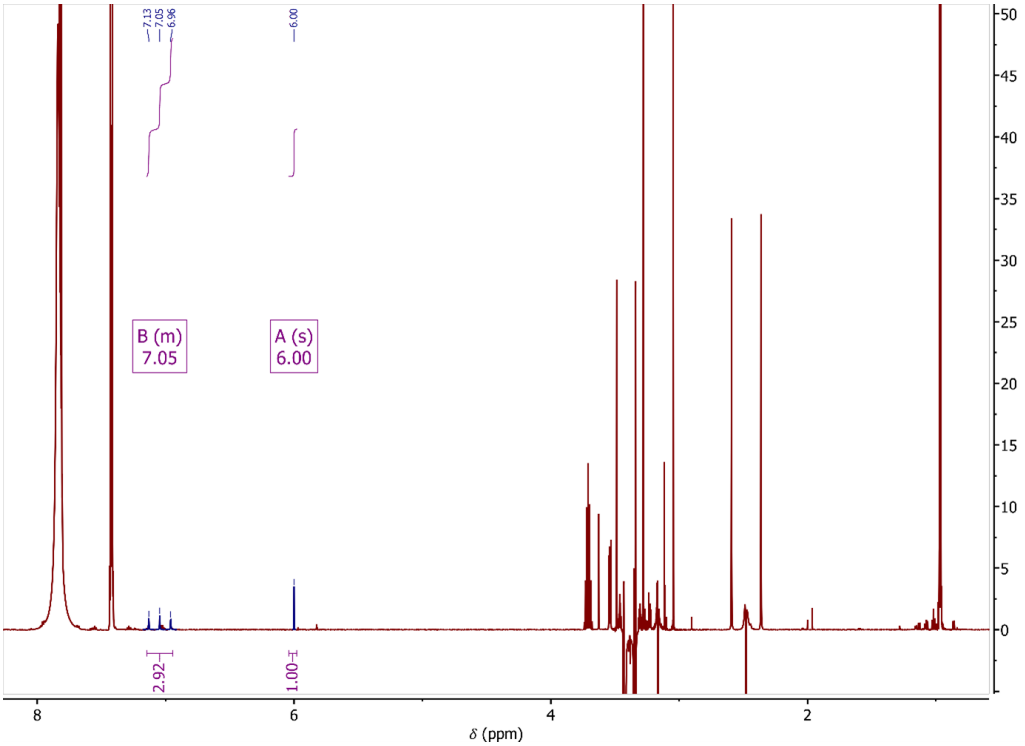

Figure S2.6: Sample spectrum of 1H NMR on an electrolyte sample containing $^{14}NH_4^+$.

The ammonium signal is a triplet at 7.05ppm, while the TMB used as a reference is a singlet at 6.00ppm. The NMR solvent is DMSO-D_6.

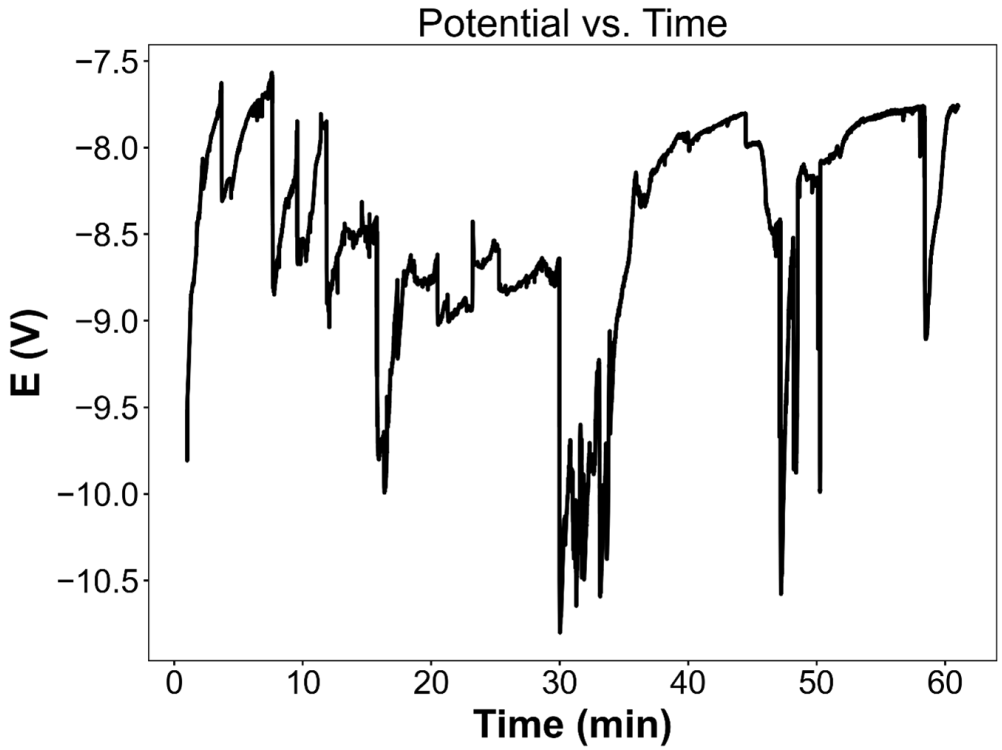

Figure S2.7: Chronopotentiogram of a typical experiment at standard conditions. Conditions: 1M NaOTf, 0.2M naphthalene, 0.1M $Ti(O^iPr)_4$ in diglyme, stainless steel working electrode, Pt counter electrode, -54 mA cm^{-2}.

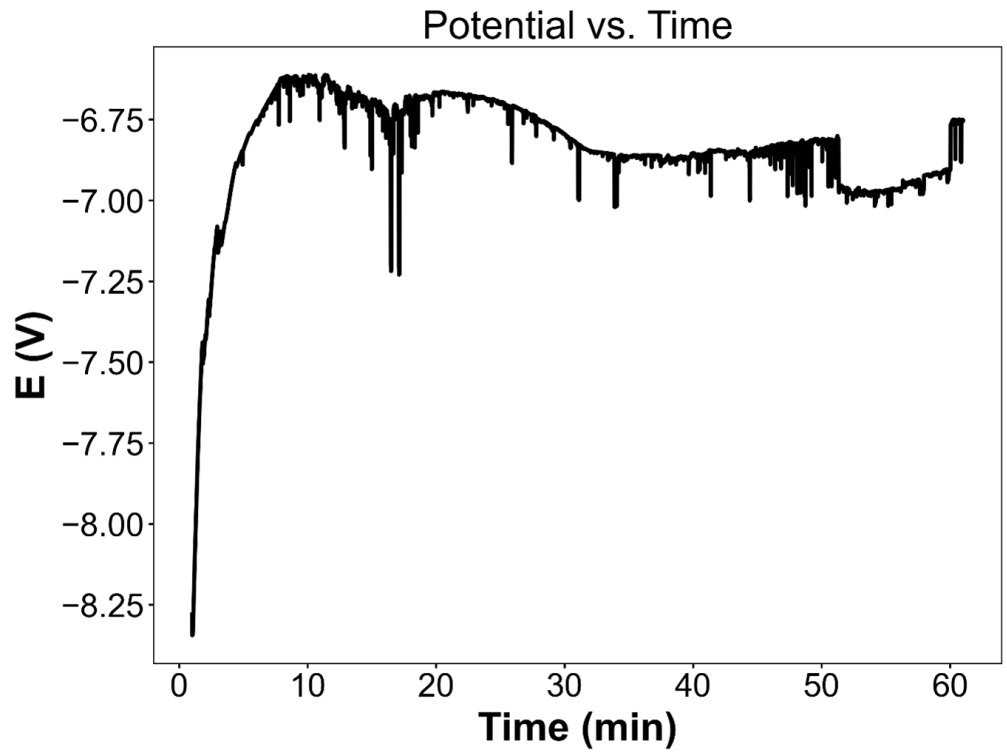

Figure S2.8: Chronopotentiogram of a no-Ti control experiment. Conditions: 1M NaOTf, 0.2M naphthalene in diglyme, stainless steel working electrode, Pt counter electrode, -54 mA cm^{-2}. As can be seen from the scale bar, when Ti is not present, the overall cell potential stabilizes significantly compared to our standard conditions.

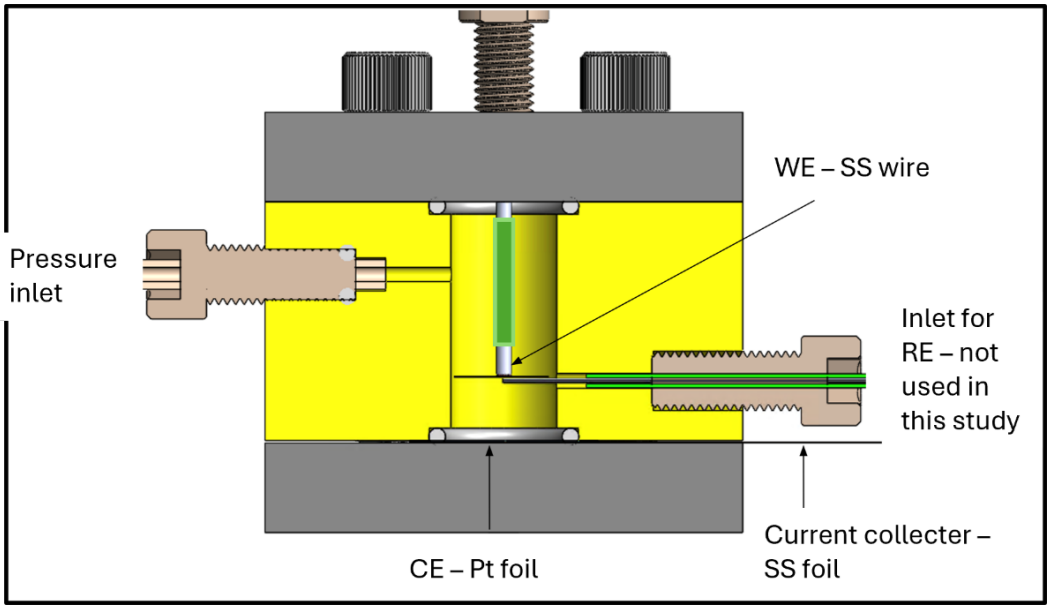

Figure S2.9: Side-on view of high-pressure cell.

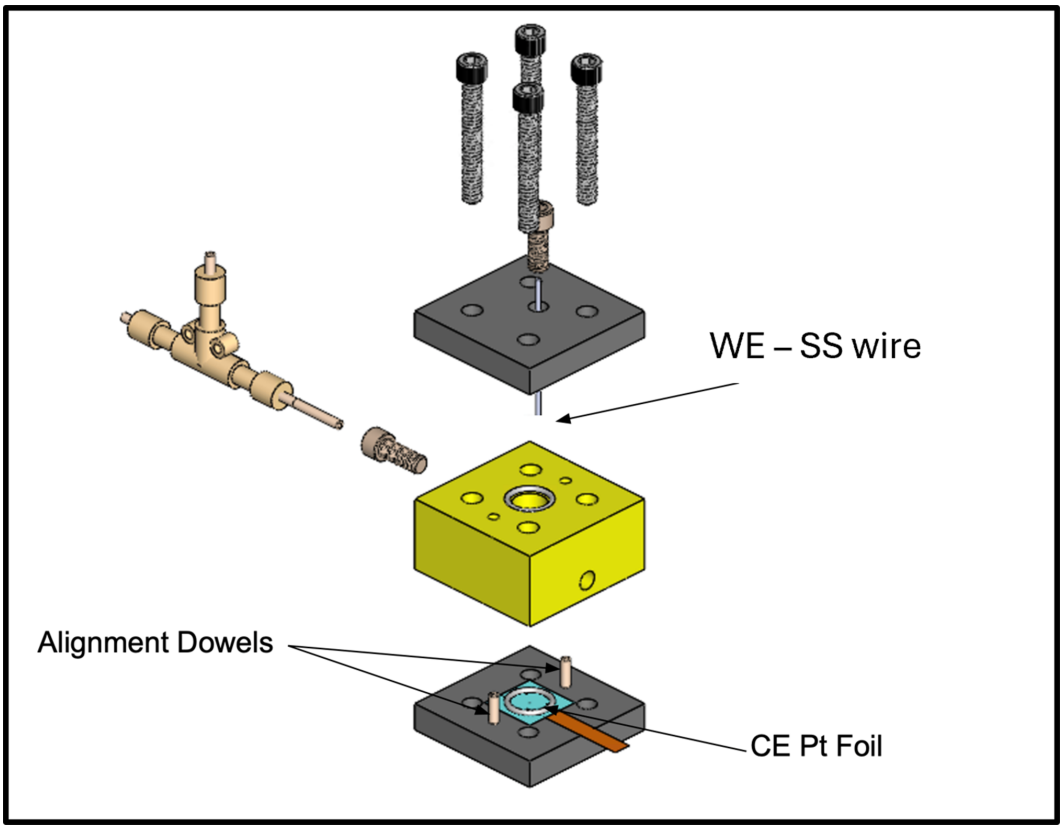

Figure S2.10: Exploded view of high-pressure cell.

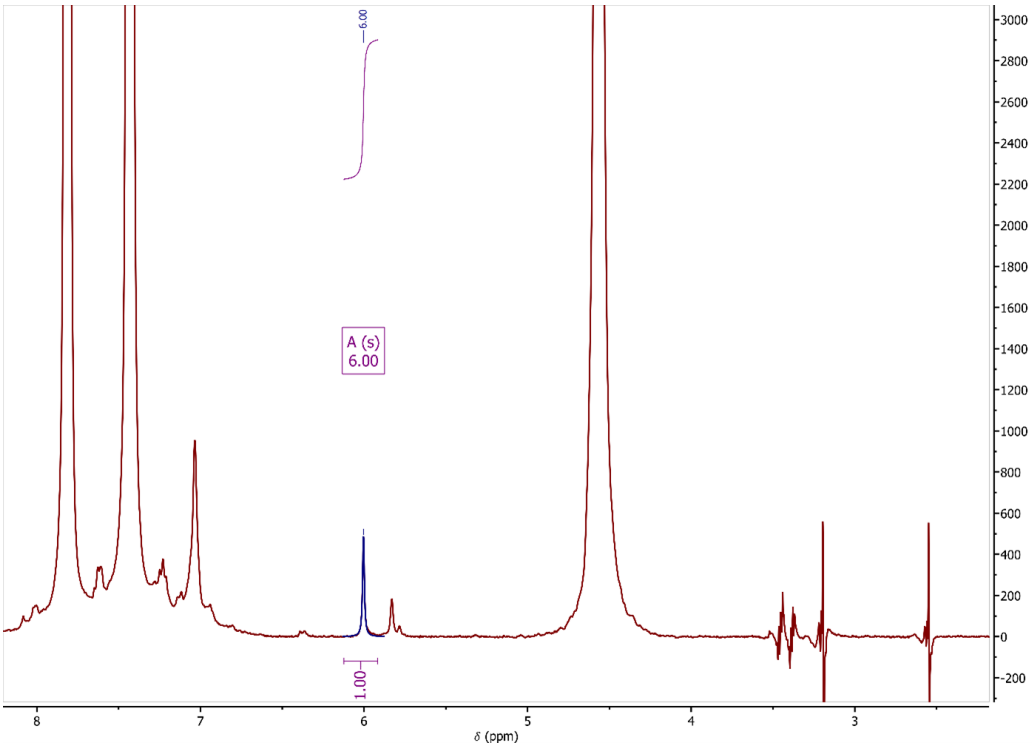

Figure S2.11: Sample spectrum of 1H NMR on blank electrolyte sample. The TMB used as a reference is a singlet at 6.00ppm. The NMR solvent is DMSO-D_6.

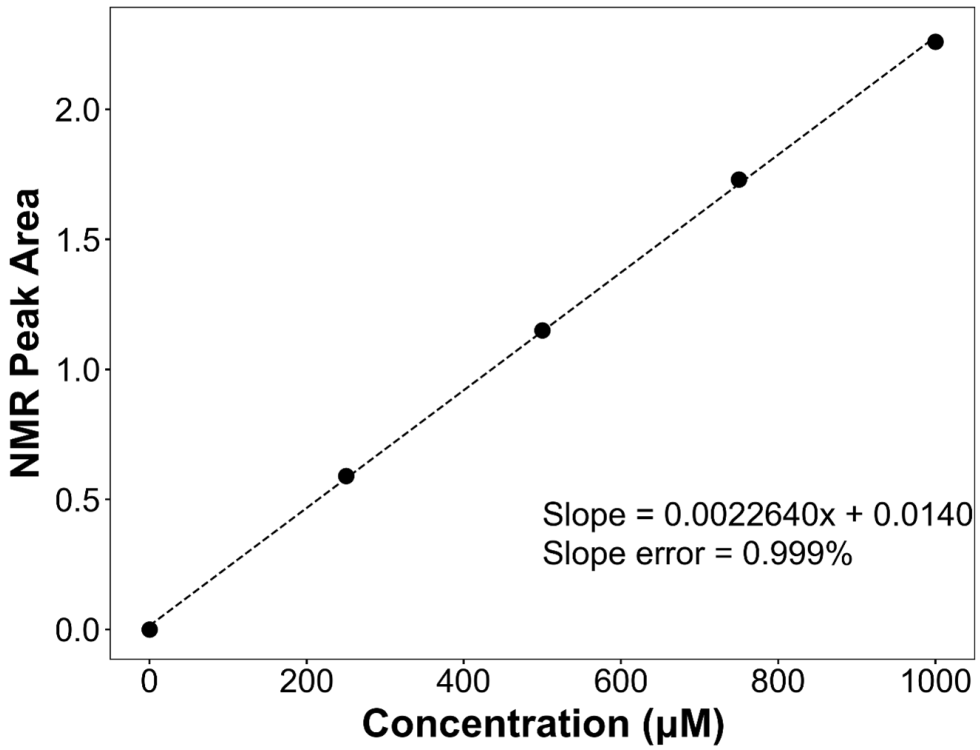

Figure S2.12: Plot of NMR peak area vs. $^{15}NH_4^+$ concentration (μM) with fresh rather than used electrolyte.

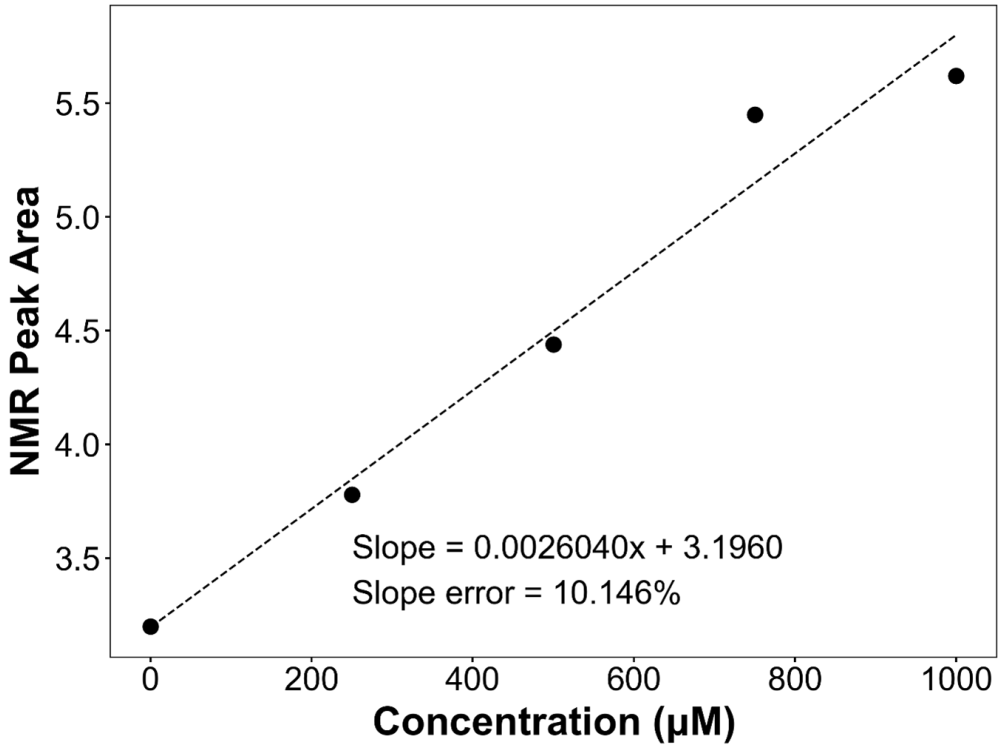

Figure S2.13: Example plot of NMR peak area vs. $^{15}NH_4^+$ concentration (μM) used to determine the yield and experimental error of ^{15}N experiments.

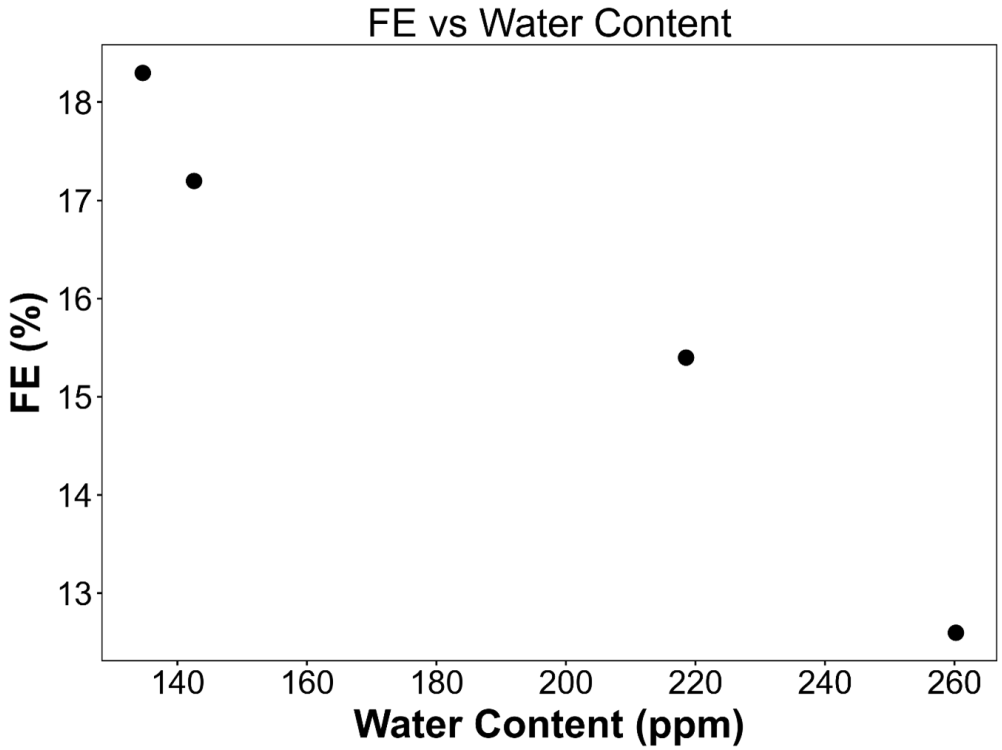

Figure S2.14: Faradaic efficiency using a representative electrolyte (1M NaOTf, 0.2M naphthalene, 0.1 M $Ti(O^iPr)_4$ in DG) vs the water content of that electrolyte.

Supplementary Tables

Condition	FE	Electrolyte ammonia concentration (mM)	Total moles of ammonia (μmol)	Yield vs Ti (%)
Standard conditions	16.7% ± 3.2%	7.4 ± 1.4	12.5 ± 2.4	7.4% ± 1.4%
No naphthalene	2.8% ± 0.2%	1.2 ± 0.1	2.1 ± 0.2	1.2% ± 0.1%
No N_2	0.2% ± 0.0%	0.1	0.15	0.1%
No naphth or Ti	0.1% ± 0.1%	0.04 ± 0.04	0.07 ± 0.07	0.0%
No current	0.0%	0	0	0
No Ti	0.0%	0	0	0
No Na	0.0%	0	0	0
High rate experiment	23.9% ± 1.0%	17.8 ± 0.7	30.2 ± 1.3	25.3% ± 1.1%
$^{14}N_2$, -120 mA cm^{-2}	14.3% ± 1.9%	6.3 ± 0.8	10.7 ± 1.4	6.3% ± 0.8%
$^{15}N_2$, -120 mA cm^{-2}	17.1% ± 0.8%	7.5 ± 0.4	12.8 ± 0.6	7.5% ± 0.4%
$^{14}N_2$, -54 mA cm^{-2}	11.4% ± 1.4%	5.0 ± 0.6	8.5 ± 1.0	5.0% ± 0.6%
$^{15}N_2$, -54 mA cm^{-2}	9.88% ± 1.0%	4.4 ± 0.44	7.4 ± 0.7	4.4% ± 0.4%
$^{14}N_2$, -54 mA cm^{-2}, 0.4 M naphthalene	10.9% ± 1.4%	4.8 ± 0.6	8.1 ± 1.0	4.8% ± 0.6%
$^{15}N_2$, -54 mA cm^{-2}, 0.4 M naphthalene	12.9% ± 1.4%	5.6 ± 0.6	9.6 ± 1.1	5.6% ± 0.6%

Table S2.1: Table of data from key experiments presented in Chapter 2. Top 7 rows: conditions presented in Fig. 2.2a. Eighth row: key high rate experiment (this was run in an electrolyte of 1M NaOTf, 0.07M $Ti(O^iPr)_4$, 0.15M naphthalene in diglyme; the electrodes were prepared as usual). Bottom 6 rows: data from conditions presented in Fig. 2.2c.

Chapter 3

A POTASSIUM-TITANIUM CASCADE ENABLES HIGH RATES FOR ELECTROCHEMICAL NITROGEN REDUCTION TO AMMONIA

This chapter is temporarily embargoed.

Chapter 4

TOWARDS A DEEPER UNDERSTANDING OF ELECTROCHEMICAL TITANIUM-MEDIATED NITROGEN REDUCTION TO AMMONIA

This chapter is temporarily embargoed.

Chapter 5

CONCLUSIONS AND FUTURE OUTLOOK

In the introduction of this work, the history—mainly thermochemical—of titanium-mediated nitrogen reduction to ammonia was explored. The remainder of this work is about its electrochemical future. In Chapter 2, a model system for electrocatalytic generation of sodium naphthalenide as single-electron reductant for a nitrogen-reducing titanium complex was established. This system demonstrated facile thermochemical kinetics, with sodium plating revealing itself as the rate-determining step. Additionally, a rate comparable to state-of-the-art LiNRR was demonstrated. However, catalytic turnover was not achieved, and stability proved to be an issue, with the reaction only lasting approx. 2 hours before stopping.

In Chapter 3, electrochemical TiNRR was extended to a potassium-mediated system. In this system, we demonstrated that in situ-generated potassium metal is competent for titanium and nitrogen reduction with greater selectivity than sodium naphthalenide. Intriguingly, despite the titanium reduction presumably occurring at the electrode surface, no transport limitations were observed in this system for any of the reagents. In contrast to the sodium naphthalenide system, this reaction also occurs at ambient nitrogen pressure and with greater stability. At ambient pressure, the rate-determining step appears to involve nitrogen reduction, while at high pressure, it appears to be potassium plating. However, titanium TON > 1 was still not observed.

In Chapter 4, we attempted to achieve a fuller understanding of the mechanism of electrochemical spatially-decoupled TiNRR. In situ UV-vis analysis was performed on the NaNpTiNRR system to attempt to isolate different processes occurring; however, the system proved too complex for a zero-knowledge approach to be sufficient. A kinetic analysis based on data presented in Chapter 3 was presented, suggesting that a parasitic process involving Ti (possibly oligomerization) is likely the main competing reaction and that Ti(III) binding N_2 may be the rate-limiting step at elevated pressures. Temporal decoupling experiments revealed that potassium and titanium/nitrogen reduction are in fact spatially decoupled, while experiments focusing on addition of proton donor showed that protonation is likely not a hidden rate-determining step. Finally, a variety of alternative reductant species were tested

in this system. Most of these yielded ammonia, demonstrating the immense promise of this system to operate under a variety of conditions.

Each of the above chapters unveiled one facet of the new paradigm that is spatially-decoupled electrochemical titanium-mediated ammonia synthesis. The performance metrics and kinetic studies detailed barely scratch the surface of the possibilities of this reaction. Therefore, contemplating directions that could be taken to further explore this space, and what place TiNRR could take within a sustainable future, is a worthwhile endeavor.

TiNRR—specifically NaNpTiNRR—has demonstrated, at time of this writing, a rate towards electrochemical ammonia synthesis greater than those reported in all but one LiNRR paper.[27] However, its stability and selectivity fall far short of established LiNRR metrics.[26,28,81] Thus, the most urgent task ahead of us is increasing these metrics. However, a simple goal does not imply simple methods. Many obstacles lie between the systems demonstrated in this work and the stability and selectivity reported in state-of-the-art LiNRR methods.

By far the most difficult obstacle towards achieving improved FE and reaction longevity for electrochemical TiNRR is simply understanding. The highest TON for Ti reported in this system is 0.3, but it is not known why the Ti compound does not turn over, or why the reaction cannot continue indefinitely with the generation of more active reductant. This is in large part because the structure of the active Ti compound, and the exact mechanism of nitrogen reduction, remain unknown. It could be that one or more highly reduced Ti species bind to and reduce N_2 on their own; it could be that a Ti(III) species binds N_2 and weakens the triple bond enough such that the externally generated reductant can perform bond scission.

Determination of this mechanism is difficult due to the complexity of the system: electrochemical plating combined with multiple putatively-homogeneous thermochemical reduction steps results in a system controlled by a multitude of factors. Nevertheless, there are analytical tools that can be brought to bear, among them EPR spectroscopy, NMR spectroscopy, UV-vis spectroscopy, and X-ray crystallography. In situ quantitative EPR could be utilized to determine the oxidation state of titanium throughout the course of the reaction: Ti(IV) is, of course, not visible by EPR, while Ti(III) and, in some circumstances, Ti(II), is. Sodium naphthalenide is also EPR-active. Therefore, tracking the formation and consumption of these species over the course of the reaction could allow for greater understanding of the oxidation level of the resting and active states of the catalyst.

NMR spectroscopy is also a valuable handle for understanding this reaction. The alkoxide ligands on $Ti(O^iPr)_4$ are visible by NMR, as is naphthalene; the relative amount of these two compounds can be measured over the course of the reaction to determine the stoichiometry of their consumption. UV-vis spectroscopy is another promising method: many of the compounds of interest (notably, reduced Ti and sodium naphthalenide) are highly colored and therefore UV-active. While the initial attempts at in situ UV-vis spectroscopy detailed in Chapter 4 were unsuccessful in elucidating a reaction mechanism, the technique remains a promising method for characterizing the system, particularly once more is known about the structure of the active complex and what competing reactions are occurring. Complementing these spectroscopies are Raman and IR, by which ammonia is visible; thus, in situ Raman and IR spectroscopy could allow for real-time tracking of ammonia evolution along with changes in the organometallic complexes over time. Finally, generation and isolation of a reduced Ti-N complex and subsequent X-ray crystallograpy could allow for direct determination of at least some of the steps in the mechanism.

Thus, understanding and improving electrochemical TiNRR for future commercial purposes is by no means an intractable problem. Ti-mediated chemistry offers the significant advantages of being cheap, readily available, and earth-abundant.[86] The rates and selectivities achieved in just under two years of work on this spatially-decoupled paradigms are already comparable to results achieved after nearly a decade of focused work on LiNRR, demonstrating the promise of this type of system. Upon achievement of a stabler and more selective method for stable, selective, and fast electrochemical TiNRR, this type of chemistry could be deployed commercially very quickly using the already-existing cell designs and infrastructure for LiNRR.[87–89] This would allow for localized, cheap, and sustainable ammonia synthesis which is compatible with renewable energy and with the dream of a fully sustainable, ethical, and green society.

BIBLIOGRAPHY

(1) Nørskov, J.; Chen, J.; Miranda, R.; Fitzsimmons, T.; Stack, R. *Sustainable Ammonia Synthesis – Exploring the scientific challenges associated with discovering alternative, sustainable processes for ammonia production*; 1283146; 2016, p 1283146.

(2) Ji, P.; Atherton, J.; Page, M. I. *Organic & Biomolecular Chemistry* **2012**, *10*, 5732–5739.

(3) IEA Critical Materials Dataset, IEA, Paris.

(4) All Nobel Prizes in Chemistry, NobelPrize.org `https://www.nobelprize.org/prizes/lists/all-nobel-prizes-in-chemistry/all/` (accessed 03/16/2026).

(5) Ghavam, S.; Vahdati, M.; Wilson, I. A. G.; Styring, P. *Frontiers in Energy Research* **2021**, *9*.

(6) Appl, M. In 2011.

(7) Foster, S. L.; Bakovic, S. I. P.; Duda, R. D.; Maheshwari, S.; Milton, R. D.; Minteer, S. D.; Janik, M. J.; Renner, J. N.; Greenlee, L. F. *Nature Catalysis* **2018**, *1*, 490–500.

(8) Smith, C.; K. Hill, A.; Torrente-Murciano, L. *Energy & Environmental Science* **2020**, *13*, 331–344.

(9) Subramani, V.; Sharma, P.; Zhang, L.; Liu, K. In *Hydrogen and Syngas Production and Purification Technologies*, Section: 2 _eprint: https://onlinelibrary.wiley.com/doi/pdf/10.1002/9780470561256.ch2; John Wiley & Sons, Ltd: 2009, pp 14–126.

(10) Erisman, J. W.; Sutton, M. A.; Galloway, J.; Klimont, Z.; Winiwarter, W. *Nature Geoscience* **2008**, *1*, 636–639.

(11) Chen, J. G. et al. *Science (New York, N.Y.)* **2018**, *360*, eaar6611.

(12) Abbas, H. F.; Wan Daud, W. M. A. *International Journal of Hydrogen Energy* **2010**, *35*, 1160–1190.

(13) Liu, H. *Chinese Journal of Catalysis* **2014**, *35*, 1619–1640.

(14) Natural gas and the environment - U.S. Energy Information Administration (EIA) `https://www.eia.gov/energyexplained/natural-gas/natural-gas-and-the-environment.php` (accessed 04/01/2023).

(15) McArthur, J. W.; McCord, G. C. *Journal of Development Economics* **2017**, *127*, 133–152.

(16) Smith, C.; Torrente-Murciano, L. *One Earth* **2021**, *4*, 104–113.

(17) Climate Impacts on African Hydropower – Analysis, IEA https://www.iea.org/reports/climate-impacts-on-african-hydropower (accessed 04/01/2023).

(18) Fertilizer prices ease but affordability and availability issues linger https://blogs.worldbank.org/opendata/fertilizer-prices-ease-affordability-and-availability-issues-linger (accessed 04/01/2023).

(19) The Iran war's impacts on global fertilizer markets and food production, IFPRI https://www.ifpri.org/blog/the-iran-wars-impacts-on-global-fertilizer-markets-and-food-production/ (accessed 04/02/2026).

(20) Lazouski, N.; Limaye, A.; Bose, A.; Gala, M. L.; Manthiram, K.; Mallapragada, D. S. *ACS Energy Letters* **2022**, *7*, 2627–2633.

(21) Fichter, F.; Girard, P.; Erlenmeyer, H. *Helvetica Chimica Acta* **1930**, *13*, _eprint: https://onlinelibrary.wiley.com/doi/pdf/10.1002/hlca.19300130604, 1228–1236.

(22) Tsuneto, A.; Kudo, A.; Sakata, T. *Chemistry Letters* **1993**, *22*, 851–854.

(23) Tsuneto, A.; Kudo, A.; Sakata, T. *Journal of Electroanalytical Chemistry* **1994**, *367*, 183–188.

(24) Lazouski, N.; Schiffer, Z. J.; Williams, K.; Manthiram, K. *Joule* **2019**, *3*, 1127–1139.

(25) Andersen, S. Z. et al. *Nature* **2019**, *570*, 504–508.

(26) Du, H.-L.; Chatti, M.; Hodgetts, R. Y.; Cherepanov, P. V.; Nguyen, C. K.; Matuszek, K.; MacFarlane, D. R.; Simonov, A. N. *Nature* **2022**, *609*, 722–727.

(27) Li, S.; Zhou, Y.; Li, K.; Saccoccio, M.; Sažinas, R.; Andersen, S. Z.; Pedersen, J. B.; Fu, X.; Shadravan, V.; Chakraborty, D.; Kibsgaard, J.; Vesborg, P. C. K.; Nørskov, J. K.; Chorkendorff, I. *Joule* **2022**, *6*, 2083–2101.

(28) Zhang, Q. et al. *Science* **2026**, *391*, 724–729.

(29) Cai, X.; Fu, C.; Iriawan, H.; Yang, F.; Wu, A.; Luo, L.; Shen, S.; Wei, G.; Shao-Horn, Y.; Zhang, J. *iScience* **2021**, *24*, 103105.

(30) Bard, A. J.; Faulkner, L. R., *Electrochemical Methods: Fundamentals and Applications*, 2nd ed.; John Wiley & Sons, Ltd: 2001.

(31) Lazouski, N.; Steinberg, K. J.; Gala, M. L.; Krishnamurthy, D.; Viswanathan, V.; Manthiram, K. *ACS Catalysis* **2022**, *12*, 5197–5208.

(32) Suryanto, B. H. R.; Matuszek, K.; Choi, J.; Hodgetts, R. Y.; Du, H.-L.; Bakker, J. M.; Kang, C. S. M.; Cherepanov, P. V.; Simonov, A. N.; MacFarlane, D. R. *Science* **2021**, *372*, 1187–1191.

(33) Lazouski, N.; Chung, M.; Williams, K.; Gala, M. L.; Manthiram, K. *Nature Catalysis* **2020**, *3*, 463–469.

(34) Peled, E. *Journal of The Electrochemical Society* **1979**, *126*, 2047.

(35) Steinberg, K.; Yuan, X.; Lazouski, N.; Klein, C. K.; Manthiram, K.; Li, Y. *Imaging nitrogen fixation at lithium solid electrolyte interphases via cryo-electron microscopy*; preprint; Chemistry, 2022.

(36) Fu, X. et al. *Nature Materials* **2024**, *23*, 101–107.

(37) page, C. C. Why 2026 is a hot year for lithium, MIT Technology Review `https://www.technologyreview.com/2026/01/22/1131563/lithium-2026/` (accessed 04/04/2026).

(38) Lithium Metal price today | Historical Lithium Metal Price Charts | SMM Metal Market `https://www.metal.com/Lithium/201102250219` (accessed 10/26/2024).

(39) Vol'pin, M. E.; Shur, V. B. *Doklady Akademii Nauk SSSR* **1964**, *156*, 1102–1104.

(40) Vol'pin, M. E.; Shur, V. B. *Nature* **1966**, *209*, Number: 5029, 1236–1236.

(41) Haight, G. P.; Scott, R. *Journal of the American Chemical Society* **1964**, *86*, 743–744.

(42) Brintzinger, H. *Journal of the American Chemical Society* **1966**, *88*, 4305–4307.

(43) Brintzinger, H. *Journal of the American Chemical Society* **1966**, *88*, 4307–4308.

(44) Brintzinger, H. *Journal of the American Chemical Society* **1967**, *89*, 6871–6877.

(45) Henrici-Olivé, G.; Olivé, S. *Angewandte Chemie International Edition in English* **1969**, *8*, _eprint: https://onlinelibrary.wiley.com/doi/pdf/10.1002/anie.196906501, 650–659.

(46) Maskill, R.; Pratt, J. M. *Chemical Communications (London)* **1967**, 950.

(47) Nechiporenko, G. N.; Tabrina, G. M.; Shilova, A. K.; Shilov, A. E. *Doklady Akademii Nauk SSSR* **1965**, *164*, 1062–1064.

(48) Van Tamelen, E. E.; Pappas, S. P. *Journal of the American Chemical Society* **1962**, *84*, 3789–3791.

(49) Tamelen, E. E. v. *Pure and Applied Chemistry* **1981**, *53*, 1259–1270.

(50) Sharpless, K. B. Studies of the Mechanism of Action of 2,3-Oxidosqualene-Lanosterol Cyclase: Featuring Enzymic Cyclization of Modified Squalene Oxides, Publication Title: ProQuest Dissertations and Theses, Ph.D. Thesis, United States – California: Stanford University, 1968, 163 pp.

(51) Van Tamelen, E. E.; Boche, G.; Greeley, R. *Journal of the American Chemical Society* **1968**, *90*, 1677–1678.

(52) Van Tamelen, E. E.; Akermark, B. *Journal of the American Chemical Society* **1968**, *90*, 4492–4493.

(53) Van Tamelen, E. E.; Seeley, D. A. *Journal of the American Chemical Society* **1969**, *91*, 5194–5194.

(54) Van Tamelen, E. E.; Boche, G.; Ela, S. W.; Fechter, R. B. *Journal of the American Chemical Society* **1967**, *89*, 5707–5708.

(55) Van Tamelen, E. E.; Seeley, D. A.; Schneller, S. W.; Rudler, H.; Cretney, W. *Journal of the American Chemical Society* **1970**, *92*, 5251–5253.

(56) Van Tamelen, E. E.; Fechter, R. B.; Schneller, S. W.; Boche, G.; Greeley, R. H.; Akermark, B. *Journal of the American Chemical Society* **1969**, *91*, 1551–1552.

(57) Van Tamelen, E. E. *Accounts of Chemical Research* **1970**, *3*, 361–367.

(58) Doisneau, R. G.; Marchon, J.-C. *Journal of Electroanalytical Chemistry and Interfacial Electrochemistry* **1971**, *30*, 487–498.

(59) Nepravishta, R.; Yu, B.; Iwahara, J. *Journal of magnetic resonance (San Diego, Calif. : 1997)* **2020**, *312*, 106687.

(60) Doyle, L. R.; Wooles, A. J.; Liddle, S. T. *Angewandte Chemie International Edition* **2019**, *58*, _eprint: https://onlinelibrary.wiley.com/doi/pdf/10.1002/anie.201902195, 6674–6677.

(61) González-Moreiras, M.; Mena, M.; Pérez-Redondo, A.; Yélamos, C. *Chemistry – A European Journal* **2017**, *23*, _eprint: https://chemistry-europe.onlinelibrary.wiley.com/doi/pdf/10.1002/chem.201700152, 3558–3561.

(62) Shi, X.; Zhang, Y.; Zhong, M.; Feng, R.; Chen, Y.; Yu, L.; Wu, Y.; Wei, J.; Xi, Z. *Inorganic Chemistry Frontiers* **2023**, *11*, 207–214.

(63) Wang, B.; Luo, G.; Nishiura, M.; Hu, S.; Shima, T.; Luo, Y.; Hou, Z. *Journal of the American Chemical Society* **2017**, *139*, 1818–1821.

(64) Hanna, T. E.; Lobkovsky, E.; Chirik, P. J. *Journal of the American Chemical Society* **2004**, *126*, 14688–14689.

(65) Hanna, T. E.; Lobkovsky, E.; Chirik, P. J. *Organometallics* **2009**, *28*, 4079–4088.

(66) Hanna, T. E.; Lobkovsky, E.; Chirik, P. J. *Journal of the American Chemical Society* **2006**, *128*, 6018–6019.

(67) Maksimowski, P.; Skupiński, W. *Journal of Molecular Catalysis* **1991**, *68*, 371–378.

(68) Nakanishi, Y.; Ishida, Y.; Kawaguchi, H. *Angewandte Chemie International Edition* **2017**, *56*, _eprint: https://onlinelibrary.wiley.com/doi/pdf/10.1002/anie.201704286, 9193–9197.

(69) Van der Weij, F. W.; Teuben, J. H. *Journal of Organometallic Chemistry* **1976**, *120*, 223–228.

(70) Mullins, S. M.; Duncan, A. P.; Bergman, R. G.; Arnold, J. *Inorganic Chemistry* **2001**, *40*, 6952–6963.

(71) Duchateau, R.; Gambarotta, S.; Beydoun, N.; Bensimon, C. *Journal of the American Chemical Society* **1991**, *113*, 8986–8988.

(72) Nikiforov, G. B.; Vidyaratne, I.; Gambarotta, S.; Korobkov, I. *Angewandte Chemie International Edition* **2009**, *48*, _eprint: https://onlinelibrary.wiley.com/doi/pdf/10.1002/anie.200903648, 7415–7419.

(73) Doyle, L. R.; Wooles, A. J.; Jenkins, L. C.; Tuna, F.; McInnes, E. J. L.; Liddle, S. T. *Angewandte Chemie International Edition* **2018**, *57*, _eprint: https://onlinelibrary.wiley.com/doi/pdf/10.1002/anie.201802576, 6314–6318.

(74) Shipman, M. A.; Symes, M. D. *Catalysis Today* **2017**, *286*, 57–68.

(75) *Nature Synthesis* **2023**, *2*, 581–582.

(76) Chang, W.; Jain, A.; Rezaie, F.; Manthiram, K. *Nature Catalysis* **2024**, *7*, 231–241.

(77) Shetty, A. U.; Sankannavar, R. *Journal of Energy Chemistry* **2024**, *92*, 681–697.

(78) Sodium price today | Historical Sodium Price Charts | SMM Metal Market `https://www.metal.com/Other-Minor-Metals/201102250465` (accessed 10/26/2024).

(79) Goyal, I.; Gande, V. V.; Bhawnani, R. R.; Hamlyn, R.; Farghaly, A. A.; Singh, M. R. Magnesium-Mediated Electrochemical Synthesis of Ammonia, 2025.

(80) Tort, R.; Bagger, A.; Westhead, O.; Kondo, Y.; Khobnya, A.; Winiwarter, A.; Davies, B. J. V.; Walsh, A.; Katayama, Y.; Yamada, Y.; Ryan, M. P.; Titirici, M.-M.; Stephens, I. E. L. *ACS Catalysis* **2023**, *13*, 14513–14522.

(81) Fu, X. et al. *Science* **2023**, *379*, 707–712.

(82) Shilov, A. E. *Russian Chemical Reviews* **1974**, *43*, 378–398.

(83) Searle, P. L. *Analyst* **1984**, *109*, 549–568.

(84) Steinberg, K.; Yuan, X.; Klein, C. K.; Lazouski, N.; Mecklenburg, M.; Manthiram, K.; Li, Y. *Nature Energy* **2023**, *8*, 138–148.

(85) Hodgetts, R. Y.; Kiryutin, A. S.; Nichols, P.; Du, H.-L.; Bakker, J. M.; Macfarlane, D. R.; Simonov, A. N. *ACS Energy Letters* **2020**, *5*, 736–741.

(86) Hunt, A. J.; Farmer, T. J.; Clark, J. H., *Element Recovery and Sustainability*; The Royal Society of Chemistry: 2013.

(87) Technology https://www.nitrovolt.com/technology (accessed 04/27/2026).

(88) Jupiter Ionics, Ammonia Energy Association https://ammoniaenergy.org/organization/jupiter-ionics/ (accessed 04/27/2026).

(89) Liquium, Liquium https://www.liquium.nz (accessed 04/27/2026).